Coordination Chemistry Reviews 337 (2017) 97–111

Contents lists available at ScienceDirect

Coordination Chemistry Reviews

journal homepage: www.elsevier.com/locate/ccr

Review

Ironing out the photochemical and spin-crossover behavior of Fe(II) coordination compounds with computational chemistry

Daniel C. Ashley, Elena Jakubikova *

Department of Chemistry, North Carolina State University, Raleigh, NC 27695, United States

ARTICLE INFO

Article history:
Received 1 December 2016
Accepted 8 February 2017
Available online 11 February 2017

Keywords:
Iron chemistry
Spin crossover
Density functional theory
ab initio methodology
Spin-state energetics
Multiconfigurational methods
Light-induced excited state spin trapping (LIESST)

ABSTRACT

Effective strategies for designing Fe(II) coordination complexes with specifically tailored spin-state energetics can lead to advances in many areas of inorganic and materials chemistry. These include, but are not limited to, rational development of novel spin crossover complexes, efficient chromophores for photosensitization of dye-sensitized solar cells, and multifunctional materials. As the spin-state ordering of transition metal complexes is strongly rooted in their electronic structures, computational chemistry has naturally played an important role in assisting experimental work in this area. Unfortunately, despite many advances, accurate determination of the spin-state energetics of Fe(II) complexes still poses a remarkable challenge for virtually all applicable forms of electronic structure theory due to being controlled by a delicate balancing between correlation and exchange effects. This review focuses on some of the more notable successes and failures of modern electronic structure theory in properly describing these systems in the absence of solid-state effects. The strengths and weaknesses of using traditional wavefunction based methods and density functional theory are considered, and illustrative examples are provided to demonstrate that the modern computational chemist should make use of experimental data whenever possible and expect to utilize a combination of methods to obtain the best results. The review closes by briefly surveying some of the many interesting combined computational and experimental studies of Fe(II) chemistry that have lead to greater fundamental insight and practical understanding of this challenging class of systems.

Contents

* Corresponding author.
E-mail address: ejakubi@ncsu.edu (E. Jakubikova).

http://dx.doi.org/10.1016/j.ccr.2017.02.005
0010-8545/

1. Introduction

Transition metal complexes can serve a myriad of functions. These include, but are not limited to, chemotherapeutic agents [1–3], CO_2 activation [4–7], artificial water splitting [8–12], C–H and C–C activation [13–17], and catalysis of numerous other organic transformations [18–21]. This diversity in function is the result of stark differences in the electronic structure of transition metal complexes in contrast to the chemistry exhibited by main group elements. In many transition metal complexes, the frontier molecular orbitals (MOs), are closely spaced i.e. HOMO-LUMO gaps are small, and are frequently partially filled and degenerate. This can result in the presence of several different electronic states that are close in energy [22]. The accessibility of multiple electronic states, often of different spin, can engender complex and interesting magnetic and optical properties. Through careful design of ligand frameworks these properties at the metal center can be tuned for specific functions.

Some of the best understood, most studied and easily controlled transition metal systems are those possessing 2nd or 3rd row transition metals [16,23–28]. Most of these metals are not abundant in the earth's crust, and are relatively expensive, thus lessening their usefulness for large-scale applications. An alternative approach is to use 1st row transition metals, such as iron, which is the focus of this review.

Iron is significantly more abundant, cheaper to employ, and usually less toxic than 2nd or 3rd row transition metals [29]. On the other hand, Fe complexes generally have weaker M-L bonds than their heavier counterparts, which leads to weaker ligand fields, more accessible spin states, and greater ligand lability. While the weaker ligand field increases the complexity of these systems, it in fact gives rise to some of the more popular applications of iron complexes. For example many iron complexes are used as spin crossover (SCO) systems [30–33]. These types of applications are only possible if there is a thermally or photochemically accessible alternate spin state. Much progress has also been made in recent years to develop effective iron catalysts [34–37].

While there are many examples of synthetic and biological Fe-based catalytic systems given in several of the above references, the goal of this review is to highlight the role that the accessible and complex spin-state manifold of iron coordination chemistry plays in SCO and photochemical applications. Specifically, we will concentrate on the role that modern electronic structure theory and computational chemistry plays in characterizing and predicting these phenomena.

The goal of this review is to (1) compare and contrast the two most useful computational approaches, *ab initio* multiconfigurational methods and density functional theory (DFT), that have been applied to theoretical studies of Fe(II) complexes and (2) illustrate their usage in selected applications related to the photochemistry and SCO. A brief outline is as follows: Section 2 will review some of the basic chemical concepts and problems of interest related to SCO. Section 3 will offer a comparison of different computational methodologies, and provide literature examples describing their respective strengths and weaknesses. Finally, Section 4 will highlight recent applications of electronic structure theory to challenging systems of current interest, mostly focusing on iron complexes with polypyridine ligands (see Fig. 1).

2. Brief overview of SCO and photosensitization by iron complexes

2.1. Fundamentals of spin-crossover

When a molecule or material undergoes a change in spin state in response to external stimuli, which can be temperature,

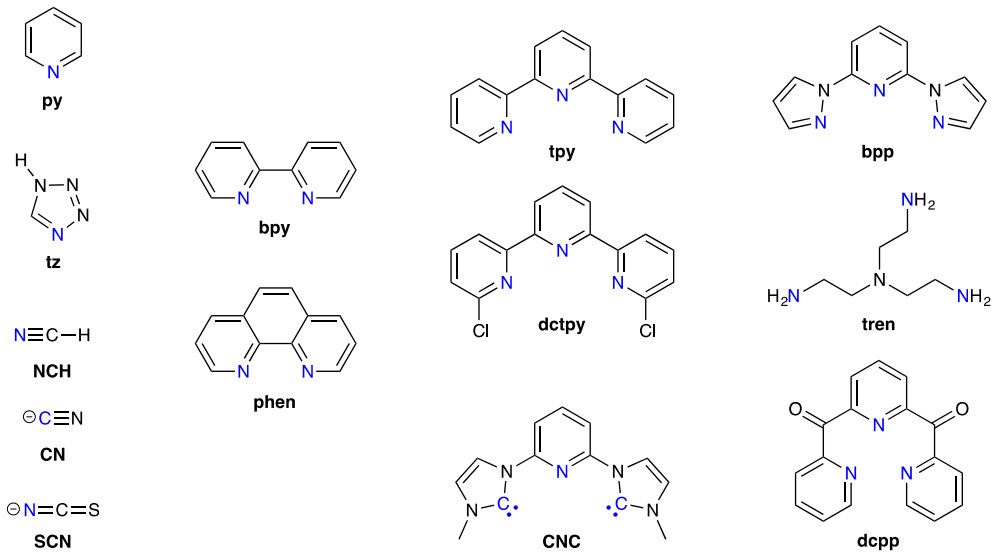

Fig. 1. Structures and abbreviations of relevant ligands.

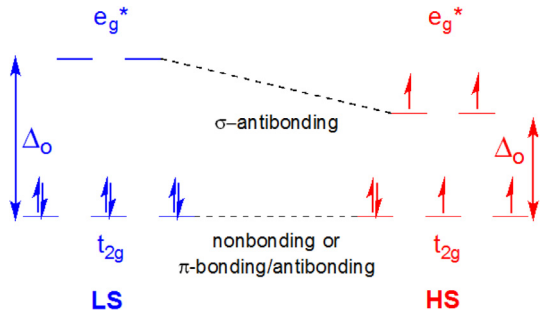

Fig. 2. Electronic configuration of singlet (LS) and quintet (HS) states of an octahedral Fe(II) complex.

pressure, or light, it is said to exhibit SCO behavior [32]. There is a wide range of potential applications of SCO. Being able to tune the spin state of a molecular unit through some easily varied physical parameter opens the door towards developing multifunctional materials [33] with possible use in spintronics [38,39]. From a chemical standpoint, changes in spin-state can lead to dramatic changes in reactivity and are often essential steps along the reaction coordinate [40]. Thus imbuing SCO behavior into catalytic systems can offer an additional method of controlling chemical reactivity. Even if a molecule does not exhibit thermally-activated SCO behavior, during the course of a chemical reaction it is possible for it to occur at higher energy points along the potential energy surface (PES) which can lead to two-state reactivity [41,42], as has been demonstrated in several synthetic and biological systems [43–45].

Arguably, the defining parameter in SCO systems is the difference in Gibbs free energy between the high spin (HS) and low spin (LS) states, $\Delta G_{HS/LS}$, defined as:

$$G_{HS} - G_{LS} = \Delta G_{HS/LS} = \Delta H_{HS/LS} - T\Delta S_{HS/LS} \quad (1)$$

This can be expressed in the usual way, as a function of enthalpic and entropic terms (Eq. (1)). When $\Delta G_{HS/LS}$ is equal to zero, the HS and LS states will be in equilibrium with each other and spin-crossover will occur. From Eq. (1) it can be seen that $\Delta G_{HS/LS}$ will be zero when the temperature is equal to $\Delta H_{HS/LS}/\Delta S_{HS/LS}$, typically referred to as $T_{1/2}$, and hence $T_{1/2}$ is one of the most commonly reported experimental measurements of SCO.

This highlights an important point regarding SCO; although microscopically SCO is clearly an electronic phenomenon, it is in fact the entropic effects that give rise to the temperature dependence. While the magnitude of $\Delta S_{HS/LS}$ will vary from system to system, it will always be positive on going to a higher spin state. One component of this derives from an increase in electronic entropy, due to an increase in multiplicity. The change in electronic entropy will only depend on the change in multiplicity, not any specific molecular features, and hence will be transferrable from system to system. For example, this value is 13.38 J K^{-1} mol^{-1} for the singlet to quintet transition [46]. A more important contribution to $\Delta S_{HS/LS}$ than this electronic effect however, is the greater vibrational entropy of the HS state [47,48]. Fig. 2 shows the electronic configuration of the singlet (LS) and quintet (HS) states of an octahedral Fe(II) complex. The quintet state has added two electrons into the antibonding e_g set of d orbitals, which will lead to a substantial weakening of the Fe–L bonds. As weaker bonds correspond to shallower minima on a PES, the spacing between vibrational levels will also decrease. At a given temperature then, the HS state will have a larger occupation of vibrational excited states than the LS state, which leads to an increase in entropy.

To obtain reasonably accurate chemical predictions of SCO behavior, computational chemists need to be able to determine both the enthalpic and entropic components. The delicate interplay between $\Delta H_{HS/LS}$ and $\Delta S_{HS/LS}$ is, in part, why predicting SCO computationally is still a formidable problem. The main challenge in the field is determination of $\Delta H_{HS/LS}$, or more specifically its electronic component, $\Delta E_{HS/LS}$. Given that experimentally $\Delta H_{HS/LS}$ is often quite small, for example ranging from ~0.7to 6.7 kcal/mol in the 30SCOFE test set [49], $\Delta E_{HS/LS}$ is often similar in magnitude to the level of error in current electronic structure calculations. Two approaches are typically taken for calculating $\Delta E_{HS/LS}$: (1) *ab initio* wavefunction based methods, frequently CASPT2 [50,51] or RASPT2 [52], or (2) DFT [53,54]. The advantages and disadvantages of both of these approaches will be discussed in Section 3.

Compared to $\Delta E_{HS/LS}$, determination of $\Delta S_{HS/LS}$ is simpler and can often be done with reasonable accuracy. Determination of vibrational entropy is usually done within the harmonic oscillator approximation, and necessitates estimation of the vibrational spacing by calculating the force constants corresponding to the normal modes of vibration. Unfortunately, in the harmonic oscillator approximation the largest errors will occur in the low-frequency modes (due to stronger anharmonic effects, and that they are generally "soft" modes), and it is these low-frequency modes that are most important in determining $\Delta S_{HS/LS}$. However, as will be discussed in detail later in this review, DFT in general manages to perform well for the determination of $\Delta S_{HS/LS}$. The standard approach then is to determine molecular geometries and vibrations using DFT, and then calculate $\Delta E_{HS/LS}$ using either DFT or an *ab initio* method [47].

An additional hallmark of SCO in solid-state systems is cooperativity; i.e., intermolecular interactions [55,56]. It is this cooperativity that leads to hysteresis in temperature-dependent magnetic measurements [57]. Unfortunately then, this feature cannot be captured in single molecule calculations, but there has been some excellent work on modeling these solid state phenomena as reported elsewhere [58–60]. Despite this, the intramolecular electronic and entropic effects that are intrinsic to a single molecule described above can still often reproduce results determined from solid-state measurements, and sometimes very simple approximations of the solid-state environment on an isolated molecule can be sufficient [46]. Given the greater relevance of the isolated molecule approach to connecting SCO to dye-sensitized solar cells (DSSCs, see below) we will neglect further discussion of solid-state systems.

2.2. Photosensitization

DSSCs are able to convert solar energy into electrical work, and as such are a potential molecular alternative to conventional silicon based solar technology. In 1991, Grätzel demonstrated that by using a mesoporous TiO_2 film sensitized with a ruthenium

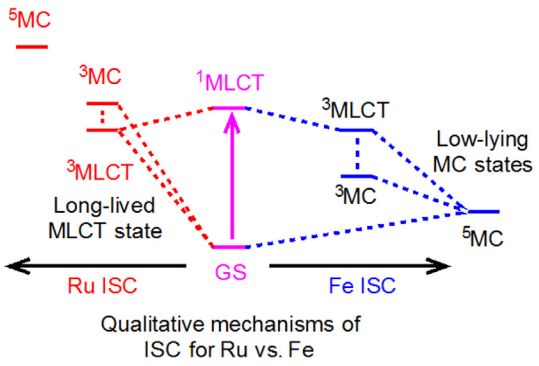

Fig. 3. Qualitative mechanism of ISC in Fe(II) and Ru(II) polypyridines.

dye it was possible to obtain an efficiency of ~8% [61]. This was a dramatic increase in efficiency from previous DSSCs and sparked a flurry of research activity in this area that is still rapidly growing today [62]. The general workings of a DSSC are as follows: Absorbance of incident light occurs at a specific molecular chromophore attached to a semiconductor surface. This excited complex can then inject an electron via interfacial electron transfer (IET) into the semiconductor, generating current. The dye is then regenerated by oxidizing an electrolyte in solution (often iodide), and the electrolyte is subsequently reduced at the cathode surface. There are numerous features that must be carefully considered to optimize the cell. One of these features is the kinetics of electron injection into the semiconductor vs. decay of the excited dye complex. These effects can be related to the quantum efficiency of the DSSC in a general way through Eq. (2) [62,63]:

$$\frac{k_{IET}}{k_{IET} + k_{ISC}} \tag{2}$$

Here k_{IET} is the rate constant associated with IET, while k_{ISC} is the rate constant associated with the collapse of the excited state back to the ground state through intersystem crossing (ISC). In the more general sense, k_{ISC} would represent all forms of decay of the excited state, however here we will focus on ISC specifically. The most successful implementations of DSSCs have employed Ru-based chromophores [64]. Part of the reason for this is that the lifetime of the MLCT state which is responsible for IET is quite long, on the order of nanoseconds, thus k_{ISC} is small compared to k_{IET} [65]. The initial excitation event generates a ^{1}MLCT state, which then undergoes ISC to a ^{3}MLCT state on the sub-ps time scale [65]. As mentioned in the introduction, there are environmental and cost considerations that make using Ru dyes undesirable, and these issues would be mitigated if they could be replaced with a 1st row metal such as Fe. Unfortunately, Fe DSSCs so far have not been nearly as successful as their heavier counterparts [63]. Due to their weaker M–L bonding, Fe complexes have much smaller ligand fields and can access metal-centered (MC) HS states that are significantly lower in energy than the MLCT state. It is the MLCT states that are active in the IET process, so while the lowest energy excited states of Ru complexes involve transfer of the electron to a ligand that is bound to the TiO_2 surface, for Fe these MLCT states can decay to the inactive MC HS state (see Fig. 3). This leads to much shorter excited state lifetimes (~100 fs [66,67]), and therefore lower quantum efficiency. Recently however, numerous Fe complexes have been synthesized that have much longer lifetimes. Wärnmark and coworkers [68–70] showed that $[Fe(CNC)_2]^{2+}$ exhibits a long lifetime of the MLCT state, which may in part originate from a larger ligand field due to strong σ-donation effects from the carbene ligands (see Fig. 1 for ligand structure) [71]. Additionally, Damrauer and coworkers demonstrated that $[Fe(dctpy)_2]^{2+}$ exhibits a long lifetime on the order of ~16 ps [72]. Interestingly, it is currently thought that this long-lived MLCT state may actually be a quintet as opposed to the typically expected singlet and triplet MLCT states. It is not yet clear how, or if, this electronic feature factors into the longer lifetimes. Wärnmark and Damrauer's work are discussed further in Section 4. Very recently, Wenger and coworkers prepared a Cr(0) complex that possesses an excited state lifetime on the ns timescale, which they propose is an analog for $[Fe(bpy)_3]^{2+}$ [73]. While this is not an Fe complex and will not be elaborated on further, it is certainly a promising development that bodes well for the application and development of effective 1st-row transition metal sensitizers.

All this demonstrates that the performance of Fe based DSSCs can be improved if the ISC (k_{ISC}) processes were to be slowed down, which is difficult to accomplish through rational molecular design unless the actual spin-state manifold of the excited states can be resolved. This then is the connecting feature between SCO applications and photosensitization. In both types of systems, it is crucial for researchers to predict the qualitative and quantitative ordering of the various electronic states, in addition to the structural and electronic features of the different species involved. It is important to note that slowing down k_{ISC} is only one strategy for improving the efficiency, another being to speed up k_{IET}. As shown in Eq. (2) what matters is the size of these rate constants relative to one another, and so optimizing IET, ISC or both are all viable approaches [63]. While most of this review will be focused on spin-state energetics, and hence SCO and ISC, Section 4.3 will briefly highlight how computational chemistry has been employed to model the IET process.

One active related area of research that neatly marries SCO and photosensitization together is light-induced excited-spin-state trapping (LIESST) [74]. The formation of the HS quintet state is typically the desired outcome in LIESST, as it allows "trapping" of the HS state often at much lower temperatures than are thermodynamically preferred. Computational and experimental studies on photosensitization, SCO, and LIESST often overlap as they are essentially all concerned with the same spin surfaces and how they interact with each other.

3. Leading computational methodologies: wavefunction theory vs. DFT

Transition metal chemistry has long posed a challenge for electronic structure theory. Unlike most main group chemistry, transition metal complexes often have several accessible and relevant electronic states, and it can be challenging to definitively determine their energetic ordering. Near-degenerate spin-states can be rationalized as a consequence of small to modest d orbital splitting, a typical feature of Werner type coordination complexes [75]. Obtaining correct spin state energies requires a delicate balancing between electron-electron repulsion, exchange interactions, and the d orbital splitting [76]. Naturally, this necessitates accurate treatment of both dynamic and static correlation effects [77]. The d orbital splitting will be even smaller for 1st row metals than 2nd or 3rd row metals due to the aforementioned weaker ligand fields, and this can lead to low-lying MC states as mentioned earlier. Relativistic effects can also become important, especially for the heavier metals. As this review focuses specifically on Fe, a relatively light transition metal, we will not extensively discuss relativistic corrections, and instead refer the reader to the literature [78,79]. It is important to note, however, that relativistic corrections should not be neglected when determining the rates of spin-surface transitions due to the importance of spin-orbit and spin-spin coupling parameters. In modern electronic structure calculations transition metal complexes are typically treated with two broad types of theory. The first of these are wavefunction methods. Specifically, *ab initio* multiconfigurational methods based on multiconfigurational self-consistent-field (MCSCF) reference wavefunctions are popular, and have come to represent the standard for accurate spin-state calculations. The other method is DFT which, in theory, is not typically as reliable as *ab initio* multiconfigurational methods (*vide infra*), can often provide valuable qualitative and quantitative insight at a fraction of the computational cost. In this section we will describe some general features of these methods and the most important issues to consider before starting a calculation yourself, or interpreting someone else's data. We will not go into extensive depth about the theory behind these, and other computational methods, as there are other resources that cover this [58,76,80–85]. In general, we will assume that the reader has general familiarity with complete active space self-consistent field theory (CASSCF), Møller-Plesset perturbation theory (MPn), coupled cluster (CC), configuration interaction (CI), and DFT.

3.1. Wavefunction methods

3.1.1. MCSCF: Choosing an appropriate active space

CASSCF is the most commonly applied MCSCF method, and works under a similar principle as CI, constructing the wavefunction as a linear combination of single-configurational wavefunctions called configuration state functions (CSFs). The critical difference is that CASSCF does not generate all possible CSFs for the entire orbital space, but rather employs a user-determined set of orbitals and electrons called the active space, within which a full CI is performed. In addition, these orbitals are also variationally optimized in response to the CI procedure; a significant difference between the CI and CASSCF wavefunctions [86].

Selection of the active space is the most critical step in a CASSCF calculation (and any subsequent calculations utilizing this wavefunction), and requires at least basic knowledge of the electronic structure of the system in question and the types of information desired from the calculation. This is generally a non-trivial problem that often requires chemical intuition, experience, and trial and error to perform correctly. While recently compelling automated methods of active space selection have been developed [87], there are also useful general guidelines provided in the literature [86,88] for choosing active spaces for a given molecule that are often sufficient, and we will go through some broad considerations relevant to transition metal complexes here. In general, frontier molecular orbitals should be included, especially if the HOMO-LUMO gap is small. If an included orbital has significant bonding interactions, then any correlating antibonding orbitals should be included as well. If excited state properties are to be determined, then any orbital that will become newly occupied in the excited state should also be included. This brings up a challenging point regarding active space design, typically it is desirable to maintain a consistent active space throughout a given study, i.e. if one is calculating the energies of various excited states they should all be calculated with the same active space. Similarly, if a bond-breaking/making process is being studied (something CASSCF is well-suited for), the bonding and antibonding orbitals should be included in the reactant/product states as well as the transition states. Often an orbital that will be important for describing the multiconfigurational character of the wavefunction in one state/structure will no longer be as important in another state/structure, and will rotate out of the active space in favor of another orbital.

With regards to transition metal complexes there are some additional considerations. All five frontier d orbitals should be included, in addition to their M–L bonding counterparts. Additionally, in many cases inclusion of an additional set of virtual d orbitals, a "double shell" is recommended to help variationally account for radial correlation effects. A general schematic of a typical active space for an octahedral Fe(II) complex is shown in Fig. 4. The double shell effect is usually more important for small, electron-rich metals, so it should be considered a necessity for 1st row transition metals with more than five d electrons, and it can also be important for accurately describing charge-transfer excitations [89]. It may be supposed that the double-shell effect can always be safely neglected if only qualitative information about the multiconfigurational wavefunction is desired, but a recent work by Gagliardi showed that this is not always the case [90]. In a study of bimetallic complexes, it was seen that the nature of the Fe-based orbitals (localized vs. delocalized) was highly dependent on whether or not the double shell effect was accounted for. As expected it also made a significant difference in determining the spin-state energetics, with the larger active spaces more accurately matching the experimentally determined spin-state ordering.

Early work by Pierloot [89] on benchmarking DFT against CASPT2 calculations for the spin-state energetics of several small model Fe(II) complexes, notably the iconic $[Fe(bpy)_3]^{2+}$, which will be discussed further below, demonstrates some of the above described features of active space design. The importance of incorporating the double-shell effect was demonstrated in that it had a large effect on the calculated energies. Additionally this study also highlighted an important practical and conceptual point regarding active space selection. Of the several small models studied, inclusion or neglect of ligand bonding orbitals did not always have a large effect, only the complexes that had significantly covalent Fe-L bonds, required inclusion of these orbitals. This reinforces a general concept that typically enhanced covalency tracks with more multiconfigurational behavior [91], and hence larger active spaces are required. Pierloot had previously demonstrated this in studies of CrF_6 and $[CrF_6]^{3-}$, where the former was much more multiconfigurational due to the increased covalent interaction between fluoride and the high-valent Cr(VI) ion [92]. Altogether, this is an important, albeit unfortunate consequence, in that in general Fe polypyridyl complexes should require larger active spaces.

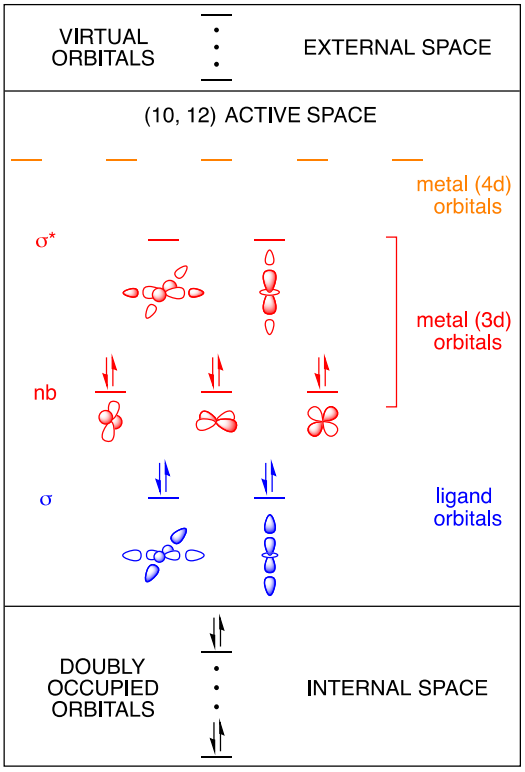

Fig. 4. Diagram of a (10, 12) active space. Note that the double shell effect is accounted for by including a set of 4d orbitals.

3.1.2. Handling large active spaces

As various *ab initio* multiconfigurational methods have been implemented over the years, they have become essentially the standard method for accurately and rigorously determining spin-state splitting in lieu of experimental evidence. In addition to providing high quality quantitative results, the CASSCF reference wavefunctions themselves are generally considered consistently reliable as qualitative electronic structure descriptors (assuming an appropriate active space is chosen), even in cases where DFT can often give varying results. One clear advantage that *ab initio* multiconfigurational methods have over DFT is that it is almost always possible to rationally and systematically improve the quality of the results through careful active space design. Unfortunately, often what is needed to systematically improve the

results is simply a larger active space, which can quickly become difficult, if not impossible, to implement with current computational resources. Additionally, appropriate treatment of dynamic correlation is not always straightforward and has many complications of its own. Numerous methods have arisen over the years to allow for *ab initio* multiconfigurational calculations with larger active spaces, notable among these are RASSCF (and its CASPT2 analog, RASPT2) and Density Matrix Renormalization Group (DMRG) methods [93–96]. Early work demonstrated that DMRG was effective for treating transition metal complex spin-state ordering [97]. Pierloot and co-workers have also seen good results when combining DMRG and CASPT2 approaches [98].

RASSCF is conceptually similar to CASSCF, except the active space itself gets divided into three regions. One of these is the same as in CASSCF, a set of orbitals in which all possible electronic configurations are considered. The other two include a set of doubly occupied and empty orbitals of which only limited numbers of excitations are allowed, thus reducing the size of the configurational space, and yielding a greatly expanded active space at a cost comparable to CASSCF. RASSCF is itself a more specific instance of general active space self-consistent field theory (GASSCF) [99], in which any number of arbitrary active spaces may be implemented. It is likely that GASSCF in combination with the newly developed GASPT2 [100], will be useful tools for calculating accurate spin state energetics as well. It should be noted however, that the additional flexibility of RASSCF and GASSCF leads to a more customizable wavefunction and greater difficulty in choosing a proper active space. Additionally, while RASPT2 certainly can be useful for calculating transition metal spin-state energetics [90,101,102], in other instances it can actually be less accurate than CASPT2 for the same total active space size [103].

In general, choosing a meaningful active space for RASSCF is potentially even more complicated than CASSCF, which was nontrivial to begin with, which brings up one of the main disadvantages of *ab initio* multiconfigurational methods: they are in no way a "black box". Design of, and convergence to, a meaningful active space often requires deep insight into the electronic structure being investigated. Even if the computational resources are available, an active space that is not thoughtfully designed and analyzed will yield useless results.

3.1.3. Accounting for dynamic correlation

Electron correlation is often divided into dynamic correlation and static correlation. Roughly speaking, dynamic correlation is related to the instantaneous coupling of an electron's behavior with the other electrons in the system, while static correlation is related to multiconfigurational behavior due to low-lying states [22]. A proper CASSCF wavefunction will be able to adequately treat static correlation, and provide an accurate qualitative picture of the electronic structure. Static correlation typically only makes up a small component of the correlation energy however, and as such CASSCF energies themselves are typically not of high quality. Additional calculations therefore need to be performed to recover the missing dynamic correlation [86]. Arguably the most well-established method of doing this is to perform CASPT2 calculations. CASPT2 uses the CASSCF wavefunction as a reference wavefunction for a multireference perturbation theory (MRPT) calculation. While there are several available flavors of MRPT, CASPT2 is likely the most popular approach and has been extensively benchmarked.

As will be demonstrated multiple times throughout this review, *ab initio* methods such as MRPT are generally able, and often necessary, to reliably calculate $\Delta E_{HS/LS}$. For example, a CASPT2 study of $[Fe(tz)_6]^{2+}$, $[Fe(tpy)_2]^{2+}$ and $[Fe(bpy)_3]^{2+}$ highlighted some of the stark differences between DFT and CASPT2, namely that DFT in general did an excellent job generating accurate molecular geometries, but couldn't reliably calculate the $\Delta E_{HS/LS}$ parameter [104]. This study also demonstrated however, that TD-DFT agreed well with CASPT2 for the calculation of excited state PESs, which is not an uncommon occurrence as will be discussed with the work of $[Fe(bpy)_3]^{2+}$ below. As TD-DFT is both significantly easier to use, and less computationally demanding than CASPT2, these results are important for future modeling studies. That being said, TD-DFT results should always be interpreted with caution, as TD-DFT has its own inherent deficiencies, i.e. no treatment of double excitations, and functional dependence issues. These deficiencies in TD-DFT further demonstrate why studies that compare the results of TD-DFT to multireference calculations and experiment are critical for its continuing application in the field.

Despite its high accuracy, there are additional technical problems with MRPT methods that have to always be accounted for. One of these is the potential of "intruder states", i.e. states that have a similar zeroth order energy as the reference state. In addition to causing discontinuities in PES generation [105], in one instance, the presence of intruder states was blamed for the prediction of the incorrect ground state for Sc_2 [106]. While it is possible in some cases to simply use a shifting procedure to remove these states, the quality of calculated results can strongly depend on what specific shifting procedure is used [105]. In the case of Sc_2 mentioned above, it was demonstrated that increasing the size of the active space was sufficient to yield the appropriate ground state [107]. In general, increasing the size of the active space will fix the more pernicious problems that plague CASPT2 [52], but obviously it will not always be possible to increase the active space especially for larger systems. Another related problem that occurs in CASPT2 calculations is that there is a systematic error which causes open-shell states to be artificially stabilized relative to closed-shell states; a serious pitfall for describing spin-state energetics. In general, this problem has been well-accounted for through modification of the zeroth order Hamiltonian itself by including an empirically determined shift parameter known as the IPEA shift [108]. This IPEA shift also helps to correct for intruder states [105].

Usually a shift of 0.25 hartrees (determined from a study on the dissociation energies of diatomics [108]) is applied, but recent work using NCH as a model for a typical nitrogenous ligand, has suggested that for Fe(II) complexes a significantly larger value of 0.5–0.7 hartrees must be used [109,110]. Indeed, this was further reiterated by Hauser in an extensive benchmarking study of both CASPT2 and DFT against high-level coupled-cluster calculations [111]. They confirmed that 0.5–0.7 hartrees was more appropriate for the $[Fe(NCH)_6]^{2+}$ complex, and an even larger value was needed to accurately treat $[Co(NCH)_6]^{2+}$. On the other hand, another study of several Fe(II) complexes showed that increasing the IPEA shift worsened agreement with experimental values, and the authors concluded then that changing the shift to 0.5–0.7 hartrees may not be generally acceptable [47]. This shows that unfortunately some empiricism needs to be included in CASPT2 applications. The study by Hauser described above also demonstrated a typical conclusion about DFT (as discussed more below), which is that while some functionals could deliver chemical accuracy to one system, there was no consistent functional that performed equally well for all of them [111]. By using their high-level data, the authors did re-parameterize the CAM-PBE0 functional to successfully reproduce results for both Co and Fe, further demonstrating the usefulness of performing DFT and *ab initio* multiconfigurational calculations in concert with each other when the opportunity arises

A final note on problems associated with intruder states and the arbitrariness of the IPEA shift, is that it can be completely sidestepped by using a different form of MRPT, N-electron valence perturbation theory (NEVPT) [112–115]. The NEVPT2 method is free of

intruder states, and additionally no modification of the zeroth order Hamiltonian is required [116]. Unfortunately, NEVPT2 has not been as rigorously benchmarked for Fe(II) complexes and spin-state energetics in general to the same extent as CASPT2, making its application in absence of experimental data difficult. However, several existing benchmarking studies do show promise for general applicability of NEVPT2 in this regard [117,118]. Additional benchmarking should be undertaken when possible to augment CASPT2 studies so the utility, or lack thereof, of NEVPT2 for Fe(II) can be ascertained [111].

It should also be mentioned that there are certainly other attractive *ab initio* methods besides MCSCF/MRPT that show real promise for becoming useful alternatives. For example, a recent study on the aforementioned $[Fe(NCH)_6]^{2+}$ model system, employing fixed node diffusion Monte Carlo (DMC), was able to obtain agreement with CCSD(T) results within ~0.3 eV for calculating $\Delta E_{HS/LS}$ [119]. Part of the challenge with DMC is the quality of orbitals used to build your initial trial wavefunction, and one of the interesting results of this study was that orbitals calculated with hybrid DFT functionals were better in this regard than HF or CASSCF-derived orbitals. This was explained as being a result of the hybrid DFT orbitals more accurately accounting for short-range correlation effects.

Some of the most intriguing alternatives to MCSCF/MRPT are methods which utilize both MCSCF and DFT to properly account for both static and dynamic correlation. One way to approach this is to treat long-range interactions (primarily static correlation) with a wavefunction based method, while simultaneously using DFT to treat short-range interactions (primarily dynamic correlation). These methods are typically referred to as WFT-srDFT where "WFT" refers to the type of wavefunction theory used for the long-range interactions. Both typical CAS and DMRG methods have been applied for the WFT method, and in general promising results have been seen for these "hybrid" methods [120,121]. Use of WFT-in-DFT embedding approaches by the Miller group, where a WFT is applied for one fragment of the system (subsystem) and DFT is used to treat the other subsystem, have demonstrated encouraging results in calculating the spin-state energetics of $[Fe(H_2O)_6]^{2+}$ when a WFT treatment is applied only to the transition metal center [122,123]. DFT has also been effectively utilized in the multi-configuration pair-density functional theory (MC-PDFT) where a multiconfigurational wavefunction is used to generate an electron density (and other density-derived parameters) which can then be treated using a density functional. Remarkably, MC-PDFT can obtain quantitative accuracy but is of approximately the same cost as MCSCF calculations without MRPT corrections [124,125]. Finally, recent work by Hohenstein has shown that great improvement in the description of excited states using CAS-CI approaches can be made by treating the core electrons of a CAS wavefunction with DFT, thereby accounting for correlation effects in the inactive space, while still maintaining an appropriate multiconfigurational description of the active space [126].

3.2. DFT

3.2.1. Efficiency vs. reliability

The high computational cost of *ab initio* methods, reliable as they often are, was a serious impediment to computational analysis of transition metal complexes, which are typically much more computationally demanding than main group systems. The development of Kohn-Sham (KS) DFT in the 1960s [53,54] and the significant advances in the quality of exchange-correlation functionals developed in the 1990s [127] dramatically changed this situation. Currently, DFT is the most common approach to handling transition metal chemistry, which is now just as computationally accessible as main group chemistry. Even studies that employ wavefunction based analysis of transition metals virtually always rely on DFT in one fashion or another (as discussed further in Section 4.1), making it an indispensable tool for the inorganic chemistry community. Indeed, some of the most cited papers in chemistry and physics are DFT papers [81,128], and DFT's combination of speed and accuracy has ensured its continuing popularity.

Certainly DFT's greatest strength is its efficiency. *ab initio* methods typically involve using a HF (or CASSCF) wavefunction as a reference wavefunction, which in and of itself, will likely only be of qualitative utility. Correlation energy is then recovered through various methods, most of which are highly expensive. DFT on the other hand requires no additional correction calculations aside from performing SCF calculations to solve the KS equations. In fact, the KS Hamiltionian is similar to the HF Hamiltonian, the difference being the presence of the exchange-correlation term. DFT calculations actually scale better than HF calculations (N^3 vs. N^4), yet can often rival *ab initio* methods in terms of accuracy. While typical KS DFT is a single-determinantal method just as HF, DFT calculations can still manage to provide reasonable results for numerous transition metal systems. Single-reference wavefunction methods are often not suitable for transition metal complexes due to the significant multiconfigurational character of these systems [129].

Unfortunately, all of DFT's problems (unreliable spin state energetics, poor accounting of dispersion interactions, and self-interaction error to name just a few) can be traced back to the fact that we do not know the correct form for the actual exchange-correlation functional. Several functionals have proven to be reasonably reliable, but none are universally appropriate for all chemical systems/properties, making DFT in generable less reliable than wavefunction methods. Therefore, a great deal of benchmarking is still continuously required to correctly make use of DFT in complex situations.

One of the most relevant shortcomings of DFT for iron chemistry, and transition metal chemistry in general, is its functional dependence for accurately describing spin-state energetics [75]. The difference in energy between spin states is chiefly due to the delicate interplay of electron pairing energy, and exchange energy as described earlier. As such, the treatment of exchange by an exchange-correlation functional is of paramount importance for accurate energetics. One highly popular method of treating this is to include some percentage of exact HF exchange into the functional, based on the adiabatic connection method [127]. Spin-state energies are highly sensitive to the degree of exact exchange incorporated [130], and it is difficult to know how much should be used *a priori* for a given system. There have been numerous studies on this problem (as discussed below), and while the problem is still significant, some clever "workarounds" have been developed outside of benchmarking against *ab initio* calculations, as detailed further in Section 4.

Overall, with careful planning, for a modestly sized system, *ab initio* multiconfigurational methods are the ideal choice for calculating accurate spin state energetics of transition metal complexes. This makes them well suited for benchmarking studies. The cost and technical complexity of *ab initio* multiconfigurational calculations however, makes DFT the only practical methodology for large-scale systems, structure determination, vibrational analysis, and systematic screening of large numbers of compounds. As mentioned earlier, one of the greatest assets of *ab initio* multiconfigurational methods is that they are more "reliable" in that they don't suffer from the functional dependence issues of DFT. In practice, however, this will only be rigorously true if the active space is appropriate, the basis set is large enough, and the proper method of dynamic correlation treatment is employed. Significant care has to be used when employing calculations from either set of these methods. In light of this, we will continue to place emphasis

on examples that demonstrate how the computational field as a whole continues to greatly benefit from both of these methods working synergistically with each other.

3.2.2. B3LYP and the effect of HF exchange*

As DFT grew in popularity and applicability, especially for many properties of transition metal complexes, there was naturally enthusiasm towards the idea that it could be used to predict challenging spin-state energetics. Unfortunately, early studies [131–136] showed just how challenging this problem would be in part due to uncertainty in predicting which approximated exchange-correlation functional would be effective for a particularly system. Early on it was observed that so-called "pure" GGA functionals generally over-stabilized LS states, while "hybrid" functionals over-stabilized HS states. Here "pure" and "hybrid" refer to the amount of HF exchange incorporated in the functional itself, a value that usually ranges between 0 and 30%. While this is, at its face, an inscrutable "technical" problem, a DFT benchmarking study by Liu showed that this dependency could actually be explained in terms of the character of the SOMO in the HS state for different functional types [137]. Ultimately these problems were especially frustrating in light of the fact that both pure and hybrid functionals were generally able to successfully predict structures of transition metal complexes.

A major breakthrough came in the early 2000s in a series of papers by Reiher which methodically demonstrated the spin-state dependence on exact exchange, and how to specifically classify systems into three different categories based on how severe this effect was [46,130,138,139]. Initially, using an archetypal SCO complex as a model, $[Fe(phen)_2(SCN)_2]^{2+}$, it was determined that when employing an "intermediary" value of 15% exact exchange within the framework of the popular B3LYP functional, which itself has 20%, excellent results were obtained for predicting the SCO energetics of this complex. This reparametrized functional was referred to as B3LYP*. This remarkably simple reparameterization has generally minor effects on other thermodynamical parameters, based on the G2 test set, compared to the significant effect it had on spin-state splittings. While it is understood that B3LYP* is also not a universally accurate functional, it still has been demonstrated to be highly successful in many varied contexts, and is still routinely used [140–145].

Reiher's work demonstrates a general paradigm for employing DFT, which is that DFT can often perform remarkably well for highly complex situations, assuming the exchange-correlation functional employed is carefully chosen/parameterized. A good example of this is the extensive work by Harvey on using DFT to model the influence of spin-state on reactivity in organometallic and inorganic chemistry [40,77,146,147]. These studies required accurate calculated energetics for spin-states and barrier heights. Moreover, the actual minimum energy crossing points (MECPs) have to be calculated to accurately model reactivity where SCO is vital. This work demonstrated that while many of the perceived failures of DFT are certainly real, for an appropriately benchmarked system, it is possible to resolve complex experimental problems. As such, numerous comprehensive benchmarking studies have been performed to assess functional accuracy for spin-state energetics. A 2007 study by Casida and coworkers was particularly informative. Here 53 functionals were evaluated for calculating the vertical energy gaps on crystal structures obtained at different temperatures (and thereby reflected different spin states) for two similar Fe(II) complexes [148]. In addition to the expected findings, low HF exchange overstabilizes the LS state and high HF exchange overstabilizes the HS state, the difference between vertical $\Delta E_{HS/LS}$ energies at the different geometries was remarkably similar for different functionals. Moreover, the differences between the two complexes were quite similar across the range of functionals explored. These results generally suggested that while the spacing between spin surfaces was certainly functional dependent, the actual description of each PES was not.

Outside of determining an approximate exchange-correlation functional that always treats $\Delta E_{HS/LS}$ reasonably accurately across a broad range of complexes, computational chemists are still dependent on expensive *ab initio* calculations to determine $\Delta E_{HS/LS}$, and consequently $\Delta G_{HS/LS}$. An alternative approach has been explored by the Jakubikova group [149], where instead of focusing on the *development* of quantitatively accurate functionals, the focus was placed on the *application* of DFT, i.e. how can any DFT method be systematically applied to account for their functional dependence and still determine valuable information regarding spin-state energetics. A large series of $Fe(II)N_6$ complexes (and some non-nitrogenous ligands as well) were examined and each complex's dependence of $\Delta E_{HS/LS}$ on the %HF exchange present in the exchange-correlation functional was analyzed. As stated earlier, the observation of this effect had been known for some time, but the specific focus here was on the magnitude and consistency of this dependence. From approximately 0–25% HF exchange the relationship between %HF and $\Delta E_{HS/LS}$ was linear, and hence was characterized by the slope of this line. Most importantly it was deduced that complexes with similar average M—N bond length changes upon going from LS to HS ($\Delta R_{HS/LS}$) also displayed similar dependencies of $\Delta E_{HS/LS}$ on %HF exchange. This result agreed well with Casida's work described above [148], and strongly reinforced the idea that DFT consistently describes PES's well. By carefully quantifying the effect, and correlating it with $\Delta R_{HS/LS}$, it is then possible to determine the ground spin-state of the complex of interest by comparison to a reference molecule with a known $\Delta E_{HS/LS}$ and similar $\Delta R_{HS/LS}$ (and hence similar dependence of $\Delta E_{HS/LS}$ on %HF exchange), While this approach still does rely on either a piece of experimental or *ab initio* data, it greatly expands the utility of DFT methodology by only requiring the data for a reference compound.

A final note regarding the dependence of $\Delta E_{HS/LS}$ on %HF exchange is that while this dependence can be linear for structurally similar complexes, and hence yield reasonable trends in $\Delta E_{HS/LS}$, this is not true for comparing $\Delta E_{HS/LS}$ values for spin states of different multiplicities. Reiher showed that both $\Delta E_{T/S}$ (T = triplet, S = singlet) and $\Delta E_{Q/S}$ (Q = quintet, S = singlet) show linear dependencies on %HF exchange, but of significantly different magnitudes [138]. $\Delta E_{Q/S}$ was more sensitive than $\Delta E_{T/S}$ which can be related to a larger change in the number of unpaired electrons. This is a very intuitive but often underappreciated point, in that it means while trends in $\Delta E_{Q/S}$ and $\Delta E_{T/S}$ (and likely $\Delta E_{Q/T}$ as well) may be interpretable across a series of complexes, the relative position of the triplet and quintet states with respect to the singlet state depends on different trends for different types of $\Delta E_{HS/LS}$, and as such should be interpreted with significant care.

In addition to the factors described above, there are other factors that can have a large impact on calculated $\Delta E_{HS/LS}$ that have not been addressed in this review, and in general do not get as much attention. A recent comprehensive study by Kepp showed that dispersion and relativistic effects can be significant, ranging from ~2 to 8 kcal/mol and ~2 to 6 kcal/mol, respectively [49]. Both dispersion and relativistic corrections tend to favor the LS state. Interestingly enough, when these effects were accounted for, only B3LYP* was seen to still perform accurately. The treatment of dispersion effects is also potentially important from the standpoint of approximating solid state SCO with single-molecule calculations. In the crystalline state, each molecule will experience attractive dispersion interactions with other nearby molecules. When these additional molecules are absent it may result in the intramolecular dispersion interactions being artificially exaggerated. While much of the issue in functional selection has centered around the degree

of HF exchange incorporated, essentially the difference between hybrid functionals and GGAs, another issue is the difference between meta-GGAs and GGAs. A very recent study showed that meta-GGAs were preferable to GGAs when strong ligand fields were present, but less preferable for weak ligand fields [150]. While this demonstrates that predicting the effectiveness of meta-GGAs is far from straightforward, the connection to chemically intuitive concepts such as the spectrochemical series/bonding bodes well for intelligent application of meta-GGAs in the future.

In addition to the benchmarking studies described above it is also worth pointing out an area that has been relatively less explored, but shows potential, and that is the so-called "double hybrid" functionals [151]. These essentially incorporate effects from the virtual orbitals in a DFT calculation in a manner similar to MP2. Neese showed that the double-hybrid functional B2PLYP can be effectively used to predict the lowest energy spin state of an experimentally characterized LIESST complex [152].

3.2.3. DFT is reliable for structure determination and thermochemical corrections

One issue that can't be over-emphasized is the accuracy of DFT for determining molecular structure, and vibrational frequencies. These features are much less dependent on the choice of exchange-correlation functional than the determination of $\Delta E_{HS/LS}$. The importance of predicting molecular structure is obvious, and will not be elaborated on further, but more needs to be said about vibrational effects. Recall that it is the balance between $\Delta H_{HS/LS}$ and $\Delta S_{HS/LS}$ that determines $T_{1/2}$ (Eq. (1)). Regardless of how accurate the determination of $\Delta H_{HS/LS}$ is, if $\Delta S_{HS/LS}$ is incorrect then $T_{1/2}$ will be incorrect as well, except in the case of serendipitous error cancellation. As discussed earlier, the primary component of $\Delta S_{HS/LS}$ is the vibrational entropy component. Similarly, conversion of $\Delta E_{HS/LS}$ to $\Delta H_{HS/LS}$ requires a correction for vibrational zero-point energy (ZPE). All of these terms can in principle be generated by any electronic structure method capable of determining the force constant matrix, or Hessian, of the complex. Within the harmonic oscillator approximation, the largest frequencies will be most important for determining ZPE. This is advantageous, as the highest frequencies will correspond to the strongest bonds (steepest wells) and will likely be less susceptible to anharmonicity. Furthermore, the smaller in magnitude the frequency, the more significant small deviations become in terms of percent error. Unfortunately, while the absolute value of ZPE may be dominated by higher magnitude frequencies, $\Delta ZPE_{HS/LS}$ will be dominated by changes in the lower frequency modes [47]. The same holds true, for calculation of vibrational entropy, as it is heavily weighted towards low-frequency vibrations.

Reiher and Schneider showed [46] in a combined experimental Raman spectroscopy and DFT study that DFT was surprisingly capable of predicting accurate values of $\Delta S_{HS/LS}$. One interesting feature of their study was that there was a significant improvement of their experimental vibrational frequencies when the molecule was modeled with other pyridine rings nearby (in an attempt to affordably mimic the solid state), demonstrating that an isolated molecule approach should always be used cautiously when trying to quantitatively replicate solid state data, as all intermolecular vibrations are neglected, and these will also be low-frequency and hence important for determining $\Delta S_{HS/LS}$. Reiher's general results were also confirmed in a more recent CASPT2/DFT study on the calculation of thermal SCO parameters [47]. Several different $Fe(II)N_6$ complexes were analyzed, and by using CASPT2 to calculate $\Delta E_{HS/LS}$, and DFT to calculate $\Delta S_{HS/LS}$ and $\Delta ZPE_{HS/LS}$, accurate trends in $T_{1/2}$ were determined. The authors note that while their values of $T_{1/2}$ were not quantitatively accurate, they were accurate enough to predict the general temperature regime where the transition would occur. Part of the reason for this success is again that in general while $\Delta E_{HS/LS}$ can vary dramatically from one functional to the next, harmonic vibrational frequencies do not vary nearly as much. The interplay between $\Delta H_{HS/LS}$ and $\Delta S_{HS/LS}$, and the importance of $T_{1/2}$ suggests that perhaps $T_{1/2}$ should be what is used to calibrate DFT as opposed to $\Delta E_{HS/LS}$. This idea was tested by Yamashita [153], and showed that the dependence of $T_{1/2}$ on exact exchange is also linear, but actually significantly different from the dependence of $\Delta E_{HS/LS}$. In general, by parameterizing their functionals based on the experimentally determined $T_{1/2}$ parameter, they got excellent results for characterizing SCO systems.

A final topic to address that has been briefly mentioned above is the utility of DFT for the description of excited states via TD-DFT. While in general *ab initio* multiconfigurational methods are well-suited to describing excited states (which are often multiconfigurational regardless of whether the ground state is or not), DFT is formally a ground-state, single-determinantal method, and shouldn't be useful for excited state chemistry. The development and benchmarking of TD-DFT [154] over the last several decades has shown that this is not the case, and TD-DFT is now routinely used to predict the behavior of excited states, and for matching experimental spectroscopic measurements [155,156]. TD-DFT has naturally become very popular for characterizing transition metal complexes in place of *ab initio* methods because of the large size and complexity of these species [157]. Many benchmarking papers have been performed to determine optimal functionals to employ for organic [158] and inorganic molecules [159]. Overall, TD-DFT has emerged as an excellent alternative to *ab initio* methods, but its use still requires extensive benchmarking, and comparison to experimental data should be made whenever possible.

4. Selected applications: LIESST and photochemistry

As discussed earlier in Section 2, photochemistry, LIESST, and SCO are all related to each other by virtue of being functions of the excited electronic state manifold. In Section 3 the various pros and cons of electronic structure methods were discussed in a more general technical sense, so now we will instead focus on specific examples of applications of these methods to challenging experimental problems. These examples serve to illustrate both the importance of computational chemistry in this area, and to reinforce the general conclusions from Section 3.

4.1. Spin-state energetics and rational design of Fe(II) complexes with desired properties

Accurate determination of spin-splitting energies in Fe coordination compounds is one of the most sought-after applications of computational chemistry in this field, as it opens up possibilities for rational design of thermal SCO complexes with a specific $T_{1/2}$, as well as chromophores with large ^1A-^5T gaps and long-lived MLCT states. Therefore, over the past two decades, numerous benchmarking studies utilizing both wavefunction-based and DFT methods were devoted to this problem [89,111,130,138,139,149,160–165]. These studies established the general utility of *ab initio* multiconfigurational methodologies, especially CASPT2, for accurate calculation of spin state energetics in pseudooctahedral Fe(II) complexes [89,164] and laid a foundation for the utilization of DFT methodologies for accurate calculation of trends in spin splitting energetics [149,161]. In general, computational studies of iron coordination compounds work best when utilized for calculations of trends in a series of related complexes, where at least one of them is experimentally known and can serve as the benchmark complex [149]. This strategy was successfully used to extract useful insights into the electronic structure of SCO compounds, explain experimental observations, as well as provide guidance

for experimental design of new iron-based chromophores, as described below.

4.1.1. Insights into the electronic structure of Fe coordination compounds

Domingo et al. employed CASPT2 and CCSD(T) methodologies for calculations of a series of Fe(II) complexes with model ligands with different σ donation strengths (H_2O, NH_3, NCH, NCS, CO, PH_3), with the aim to analyze the multiconfigurational wave function within a valence bond picture [129]. Their analysis revealed a direct relationship between the weight of the ligand-to-metal charge transfer configurations in the multideterminantal wavefunction and the relative stability of the low-spin and high-spin states. Moreover, multiconfigurational character of the wavefunction becomes especially important in the presence of strong σ donor ligands, no doubt related to their increasingly covalent nature as described earlier, suggesting that calculations of such complexes cannot rely on a single reference wavefunction. These results are especially interesting in light of the fact that dependence of spin-splitting energies on the percent of exact exchange in the hybrid density functional is different for complexes with ligands exhibiting different σ donor strengths as pointed out by Pierloot and Vancoillie [89,164] as well as Bowman and Jakubikova [149]. While complexes where ionic bonding dominates (weak σ donors, small distortions in M—L bond lengths going from low-spin to high-spin) have a weak dependence on the amount of exact exchange, complexes with more covalent metal-ligand bonds (strong σ donors, large distortions in M-L bond lengths going from low-spin to high-spin) display a strong dependence on this parameter. Later work of Ioannidis and Kulik [162] revealed that increasing the exact exchange in the DFT results in the 3d electron delocalization onto the ligand and thus changes the description of the metal-ligand bonding in the complex. All of this work further illustrates that the functional dependence of calculated spin-state energetics need not, and perhaps should not, be treated as a technical issue, but rather a problem that can be resolved through chemical concepts.

As such, the intrinsic difficulties of DFT to consistently describe spin splitting energetics in transition metal complexes with a wide range of σ and π bonding interaction strengths may be connected to the changes in the multiconfigurational character of the wavefunction across this range. While it is possible to find an "ideal" value of the exact exchange parameter that will work with a particular functional and a set of complexes with ligands that display similar σ donor strengths as was done with the B3LYP* functional by Reiher and coworkers [130], this approach does not offer a pathway toward the construction of a universal DFT functional that will work for all types of iron complexes equally well. Moreover, since the dependence of spin-splitting energies on the exact exchange changes with the covalency of metal-ligand bonds, any DFT study that aims to compare spin state energies across a series of first-row transition metal compounds needs to first establish that the calculated spin splitting energies are indeed comparable across the set of complexes investigated. This can be done by either (1) confirming that the slope of the dependence of spin-splitting energies on the exact exchange in the DFT functional is similar for all complexes in the set, (2) establishing that the distortions in metal-ligand bond lengths between high-spin and low-spin structures are similar for all complexes in the set, or (3) showing that all complexes in the set have ligands with similar σ donor strength [129,149].

4.1.2. Systematic and joint experimental/computational studies of Fe (II) complexes

As mentioned in Section 3, systematic studies utilizing a combination of DFT to obtain structure and vibrational frequencies and CASPT2 to obtain electronic energies were performed by Sousa and coworkers to obtain reliable values of $T_{1/2}$ for a series of thermal SCO Fe(II) complexes with mono-, bi-, and tridentate ligands [47]. Halcrow, Deeth and coworkers have employed DFT calculations at the BP86 level of theory to probe the relationship between the bpp ligand substituents and the SCO character of Fe(II) complexes and found good qualitative agreement between calculated and experimentally observed trends [166].

One of the problems of current interest that could greatly benefit from the development of accurate approaches to calculation of spin-state energetics is the development of Fe-based chromophores with long-lived MLCT states that can be used as sensitizers in DSSCs. Prototypical Fe(II)-polypyridine complexes such as $[Fe(bpy)_3]^{2+}$ and $[Fe(tpy)_2]^{2+}$ are inefficient as sensitizers since the initially excited photoactive MLCT states undergo ultrafast ISC into the low-lying ligand-field MC states, especially $^5T_2$ (see Fig. 3 and Section 2 for additional discussion). The basic premise is to design complexes with ligand field strengths large enough to stabilize the ^{3}MLCT states with respect to the non-photoactive metal-centered triplet and quintet states. The lowest energy ligand-field state in such complexes will be the $^3T_1$, as opposed to the $^5T_2$ state (see Fig. 5).

Dixon [167–169] as well as Jakubikova [71,170] and coworkers have performed several systematic DFT studies on different series of Fe(II) complexes to determine the ligand motifs that have the greatest potential to increase the ligand field strength. These studies suggested that complexes with Fe–C bonds utilizing carbene or aryl ligands will lead to the greatest increase in the ligand field strength. While Fe(II) complexes with N-heterocyclic carbene ligands were reported at around the same time in an independent work by Wärnmark and coworkers [68] and have been since shown to display favorable photophysical properties, such as increased lifetime of the photoactive MLCT states [69] and efficient electron injection into the semiconductor [70], synthesis of Fe(II) complexes with aryl ligands has not yet been realized. Electronic structure calculations performed by Persson and coworkers at the DFT and TD-DFT levels of theory utilizing the parameterized B3LYP* functional were crucial in obtaining a better understanding of the excited-state dynamics of Fe(II) complexes with the carbene ligands synthesized by the Wärnmark group [69].

McCusker and coworkers have recently designed a new type of Fe(II) polypyridine chromophore that approaches the $^5T_2/^3T_1$

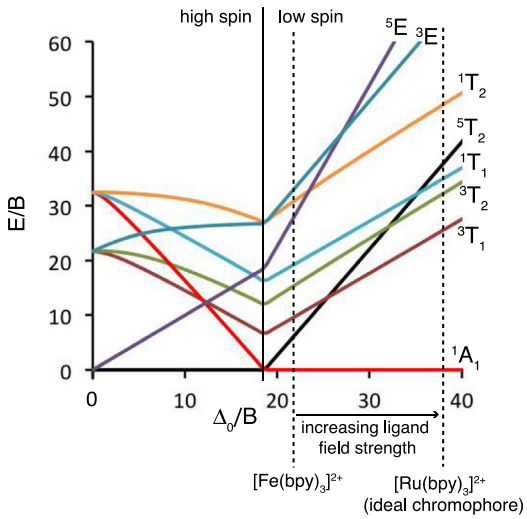

Fig. 5. Tanabe-Sugano diagram for an ideal octahedral transition metal complex with d^6 configuration, showing the impact of the ligand field strength on the ordering of various ligand-field electronic states.

crossing point (see Fig. 5) by improving the octahedral symmetry around the metal center utilizing a tridentate dcpp ligand [171]. The near-perfect octahedral symmetry in the first coordination sphere of the resulting $[Fe(dcpp)_2]^{2+}$ complex, coupled with the low-energy nature of the ligand's π^* orbitals, results in a complex with stronger ligand field strength than that of $[Fe(bpy)_3]^{2+}$ or $[Fe(tpy)_2]^{2+}$. The increased ligand field strength of $[Fe(dcpp)_2]^{2+}$ was later confirmed by electronic structure calculations [170].

An unconventional approach to reaching the long-lived MLCT states in Fe(II) complexes was taken by Damrauer and coworkers, who designed a highly-strained $[Fe(dctpy)_2]^{2+}$ complex, in which the two terpyridine ligands were substituted at 6 and 6″ positions by Cl atoms [72]. While the bulky substituents resulted in a significant decrease of the ligand field strength of the complex, stabilizing the quintet ground state, this structural change resulted in a more than 100-fold increase in the lifetime of the excited ^{5,7}MLCT states compared to $[Fe(bpy)_3]^{2+}$. Computational studies at the DFT and TD-DFT levels of theory, reported along the experimental findings, were important in gaining a deeper understanding of the ground and excited electronic structure of this complex.

Finally, a recent joint experimental and computational study by Zhang et al. demonstrated that the $[Fe(CN)_4(bpy)]^{2-}$ complex displays a long-lived MLCT state with a ~20 ps lifetime without undergoing spin crossover. Here, DFT calculations at the PBE0/6-311G(d,p) level of theory were employed to map the excited state potentials for $[Fe(CN)_4(bpy)]^{2-}$ to confirm destabilization of the ^{3,5}MC states in support of the X-ray free-electron laser and Kβ hard X-ray fluorescence spectroscopy studies with femtosecond time-resolved UV–visible absorption spectroscopy employed to characterize the excited state dynamics of this complex [172].

Overall, these specific examples illustrate that electronic structure calculations are most powerful when utilized in tandem with experimental studies to explain, corroborate, or predict the experimental results. In this case, even flawed, more approximate methodologies based on DFT and TD-DFT calculations are able to provide helpful information and the guidance needed for understanding and later applying the results of the experimental work.

4.2. Excited states and LIESST

An important application of computational studies is providing detailed understanding of photoexcited processes in Fe coordination compounds. One of the first such applications, that helped to establish the CASPT2 method as an accurate tool for calculations of electronic spectra of transition metal complexes, was a systematic study of ligand field excited states in a series of metal hexacyanometalate complexes by Pierloot et al. [173]. More recently, Formiga et al. utilized the same methodology to obtain ligand-field and charge-transfer spectra of a series of $[Fe(CN)_5L]^{n-}$ (L = *N*-heterocyclic ligand) complexes in various solvents [174].

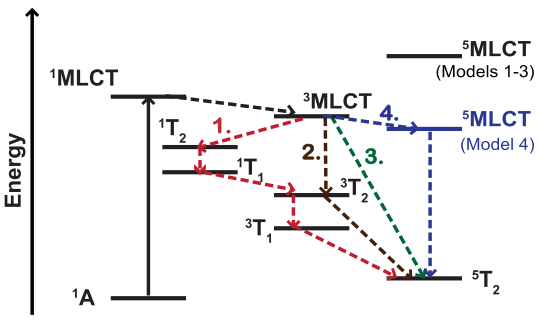

Fig. 6. Models for the ^{1}MLCT → $^5T_2$ LIESST (or ISC) process in a Fe(II)-polypyridine complex. Reproduced with permission from reference 189. Copyright 2015 American Chemical Society.

They suggested that implicit solvation effects should be included in the DFT optimizations as they improve the calculated structures, although the precise choice of solvent is not important. They also showed that while the ligand-field states are relatively insensitive to the solvent environment, the proper description of charge-transfer transitions requires the inclusion of solvent into the computational model, ideally by including the solvent molecules explicitly, whereas the polarizable continuum model is only able to partially account for the solvent effects in these systems. Overall, these studies illustrate that CASPT2 is capable of describing electronic spectra of pseudooctahedral iron complexes with excellent accuracy, within 1000 cm^{-1} of the experimentally observed transitions.

Another good example of the utility of CASPT2 and DFT methods is their application to understanding the mechanism of the LIESST process in a variety of Fe(II) compounds. Foundational experimental studies elucidating the decay pathway from the initially excited ^{1}MLCT states have been done in the McCusker research group, who studied the ISC phenomenon in the tren-based polypyridine model complexes $[Fe(tren(py)_3)]^{2+}$ and $[Fe(tren(6\text{-Me-}py)_3)]^{2+}$ [66,175–177]. Over the years, multiple models have been proposed for the ISC from the initially excited ^{1}MLCT states into the lowest energy $^5T_2$ state in pseudooctahedral Fe(II) complexes (see Fig. 6).

One of the first models suggested the involvement of the ^{3}MLCT as well as ^{1,3}T states in the cascade: ^{1}MLCT → ^{3}MLCT → ^{1,3}T → ^{5}T (Fig. 4, Model 1, red pathway) [177]. While the involvement of the ^{3}MLCT state in the cascade is well-characterized and it has been shown that this state is populated in both $[Fe(bpy)_3]^{2+}$ and $[Ru(bpy)_3]^{2+}$ complexes within 20 fs upon the population of the ^{1}MLCT state [178], involvement of ^{1,3}T states in the cascade is less clear. On one hand, these states lie energetically between the ^{1}MLCT and ^{5}T states, so their involvement might be expected. On the other hand, later studies of LIESST in $[Fe(bpy)_3]^{2+}$ employing ultrafast X-ray absorption spectroscopy suggest a simpler ISC cascade, involving only the ^{3}MLCT and ^{5}T states: ^{1}MLCT → ^{3}MLCT → ^{5}T (Fig. 6, Model 3, green pathway) [179]. The sub-picosecond time scale (<250 fs) of the entire process and recent theoretical studies predicting the crossing of the ^{5}T and MLCT bands in the Franck-Condon region seem to confirm this simpler, two-step cascade process [180].

Another theoretical model suggests a decay cascade involving the ^{5}MLCT state, ^{1}MLCT → ^{3}MLCT → ^{5}MLCT → ^{5}T (Fig. 1, Model 4, blue pathway) [181,182]. This model is, however, not supported by the available experimental and other theoretical evidence and is therefore unlikely. This does not mean, however, that the ^{5}MLCT should always be discounted in every system, as discussed earlier with respect to Damrauer's work [72]. Experimental studies of the $[Fe(bpy)_3]^{2+}$ complex based on femtosecond resolution X-ray fluorescence spectroscopy indicate that the ISC crossing occurs via the ^{1}MLCT → ^{3}MLCT → ^{3}T → ^{5}T cascade (Fig. 1, Model 2, brown pathway) [67,183,184]. Finally, recent ultrafast photoemission spectroscopy work demonstrated that in fact both sequential and direct deactivation mechanisms (Models 2 and 3 respectively) occur simultaneously for $[Fe(bpy)_3]^{2+}$, with sequential pathways being preferred over direct pathways in a 4.5:1 ratio [185]. Obviously, the details of the ISC process in Fe(II)-polypyridines are still an open question. However, both experimental and computational studies of Fe(II)-polypyridines suggest that the ISC process is initiated by the ^{1}MLCT → ^{3}MLCT step, and that crossing of the PESs of the MLCT and ^{5}T (or ^{3}T) states in the Franck-Condon region is one of the factors contributing to the ultrafast time scale of this phenomenon. Finally, recent work by Zhang et al. convincingly established the presence of ^{3}T intermediate in the ISC cascade [67].

From the computational standpoint, investigation of LIESST in Fe(II)-polypyridine complexes was tackled by a number of research

groups, mostly through construction of PESs along the relevant coordinates. Due to the complexity and the large size of the transition metal compounds, most of the PESs reported in the literature are constructed along one or two coordinates, with the Fe-ligand distance being one of them. Ordejon, de Graaf, and Sousa employed CASSCF/CASPT2 to construct one-dimensional PESs along the symmetric Fe-N_6 stretching mode for the $[Fe(tz)_6]^{2+}$ complex, that can be considered a representative for a large number of Fe(II) SCO complexes with a FeN_6 core [186]. Their work identified the $^1T_1$-$^5T_2$ intersystem crossing in the Franck-Condon region, and proposed that the deactivation of the initially excited state proceeds either through the overlap of vibrational states with an intermediate triplet state, or via an ISC process along an asymmetric vibrational mode.

CASPT2 was also utilized to analyze complex mechanistic issues in the photodeactivation of $[Fe(bpy)_3]^{2+}$. As mentioned earlier, $[Fe(bpy)_3]^{2+}$ is a prototypical Fe(II) polypyridyl complex and hence has been thoroughly investigated experimentally and computationally as a general model of ISC and LIESST processes [67,178,183,184]. A series of papers by de Graaf and Sousa on the spin-state manifold of $[Fe(bpy)_3]^{2+}$ has illuminated several points regarding the proposed mechanisms of LIESST [180,187,188]. The metal-based quintet and triplet state(s) do cross the photoexcited MLCT state (note that singlet and triplet MLCT states are essentially isoenergetic, due to very weak interactions between the metal center and bipyridyl ligand) in the Franck-Condon region, and based on this alone decay to either state is energetically plausible. However, these studies pointed out that even though the surfaces favorably cross for the ^{1}MLCT and ^{5}MC states, the spin-orbit coupling (SOC) between the MLCT and quintet state is very low, due to the change in occupancy of two electrons (double excitation) on going from ^{1}MLCT to ^{5}MC [180]. Coupling with the ^{3}MC states is much higher, and additional work suggested that decay of the ^{3}MLCT state through a cascade of metal-centered triplet states is much more likely than direct conversion to the quintet [188].

The work of Pápai et al. utilized CASPT2, along with the DFT and TD-DFT methods, to construct PESs for $[Fe(tz)_6]^{2+}$, $[Fe(bpy)_3]^{2+}$, and $[Fe(tpy)_2]^{2+}$ [104]. In addition to constructing PESs along the symmetric Fe-N_6 stretching mode for all three complexes, they pointed out that the spin-state transition in the $[Fe(tpy)_2]^{2+}$ complex cannot be described properly along a single coordinate based on the uniform lengthening of Fe—N bond lengths. Therefore, they presented PESs for the lowest energy singlet, triplet, and quintet states of this complex, evaluated along the Fe—N(axial) bonds and NNN angle of the three pyridine rings of the tpy ligands. Later on, Nance et al. argued that a third coordinate, corresponding to the tpy ligand rocking motion should be included in the PES construction for this complex [189]. The three-dimensional PESs constructed in their work revealed the presence of large low-energy valleys along the tpy rocking coordinate near the important MECPs and minimum energy crossing seams. The presence of such shallow regions suggested that low frequency ligand motions may play an important role in facilitating the ISC, and controlling this "gentle" ligand motion may provide an additional handle for controlling spin-state transitions in this and related complexes.

Finally, recent work by Canton and coworkers demonstrated through X-ray absorption spectroscopy and DFT calculations that the spin-state change in $[Fe(tpy)_2]^{2+}$ is not well described by bond length changes alone by showing that the spin-state conversion proceeds through a double axial bending motion of the ligands [190]. While each of these studies focused on different specific motions, all of them agree that often subtle molecular motions besides Fe—N breathing motions are potentially important for understanding the mechanisms of photodeactivation in Fe(II) polypyridyl complexes.

4.3. Calculations of Fe(II)-chromophore-semiconductor assemblies

Most of the experimental and computational work to date has focused on the rational design of efficient Fe(II) chromophores by increasing the lifetime of the photoactive MLCT states of these complexes. These efforts yielded some success in recent years and previous sections of this review describe several Fe(II) complexes ($[Fe(bpy)(CN)_4]^{2-}$, $[Fe(CNC)_2]^{2+}$, and $[Fe(dctpy)_2]^{2+}$) that display MLCT lifetimes in the 16–20 ps range [72,172,191]. The long lifetimes of the MLCT states are, however, not enough for iron coordination compounds to be successful in their role as chromophores in DSSCs. Other processes, such as efficient IET between the excited dyes and the semiconductor, slow charge recombination, and effective regeneration of the oxidized dyes by the redox mediators are equally important for construction of functional DSSCs that utilize iron chromophores [192,193]. Fortunately, computational chemistry possesses tools that allow one to investigate various aspects of the dye-semiconductor and dye-electrolyte interactions [194].

In terms of the Fe(II) sensitizers, perhaps the most explored area is investigation of the IET between the excited dyes and a TiO_2 semiconductor. As mentioned in Section 2.2, speeding up the IET rate is a complementary strategy to slowing down the ISC rate. Such investigations can be done either utilizing simple phenomenological formulas derived in the framework of Fermi's golden rule with parameters obtained based on DFT calculations [195–197], or by direct simulations of IET employing nonadiabatic quantum dynamics approaches [198]. Pastore et al. investigated the IET in $[Fe(CNC\text{-}COOH)_2]^{2+}$ sensitized solar cells, utilizing Fermi's golden rule with parameters obtained from electronic structure calculations at the B3LYP level, to estimate the electron injection rates between the excited dyes and a $(TiO_2)_{82}$ cluster representing a semiconductor [199]. Fredin et al. employed ground state DFT calculations of the $[Fe(CNC)(CNC\text{-}COOH)]^{2+}$-$(TiO_2)_{92}$ assembly at the B3LYP level to obtain insights into the IET process [200]. Their calculations indicate strong electronic coupling between the excited Fe(II)-carbene dye and the CB of TiO_2 which results in a fast initial injection rate.

Jakubikova and coworkers explored IET in a number of different Fe(II)-semiconductor assemblies, with dyes based on $[Fe(bpy)_2(CN)_2]^{2+}$, $[Fe(bpy)(CN)_4]^{2-}$, $[Fe(tpy)_2]^{2+}$, as well as cyclometalated $[Fe(tpy)_2]^{2+}$ complexes utilizing a combination of DFT, TD-DFT studies and quantum dynamics simulations [63,71,201–203]. These studies provided a theoretical explanation for the band-selective sensitization phenomenon observed by Ferrere and Gregg in $[Fe(bpy)_2(CN)_2]$-TiO_2 assemblies utilizing carboxylic acid as the anchor group [63,201,204]. The band-selectivity was attributed to the population of LUMO and LUMO+1 orbitals of the dye upon the excitation of the lower energy band. These orbitals are localized at the edge of the TiO_2 CB and thus suffer from both low driving force and a lack of available TiO_2 acceptor states. This work also showed that population of the LUMO in the $[Fe(bpy)(CN)_4]^{2-}$ complex suffers from similar problems. Moreover, the IET rate from the LUMO of the $[Fe(bpy)(CN)_4]^{2-}$ is much slower when the complex is attached to TiO_2 via the CN^- linker due to poor electronic coupling between the MLCT state of the dye and the CB of TiO_2. These results may also explain recent findings of Zhang et al. [172] which suggest that the IET in the $[Fe(bpy)(CN)_4]^{2-}$-TiO_2 assembly is inefficient despite the fact that the lifetime of the $[Fe(bpy)(CN)_4]^{2-}$ MLCT state is ~20 ps. To fully understand this issue, however, simulations of electron injection from the fully optimized ^{3}MLCT state of the $[Fe(bpy)(CN)_4]^{2-}$ would be necessary.

Another issue addressed by the work of Jakubikova and coworkers was the choice of the ideal anchoring group for attachment of Fe(II) dyes on TiO_2, as well as the optimal placement of the linker

on the polypyridine scaffold. Computational studies performed on a series of [Fe(bpy-L_2)$_2$(CN)$_2$] dyes (L = carboxylic acid, phosphonic acid, hydroxamate, catechol, and acetylacetonate) suggest that hydroxamate provides for the best electronic coupling between the excited dye and TiO_2 semiconductor [203]. The IET simulations for cyclometalated Fe(II) dyes identified the pyridine ring of the cyclometalated terpyridine ligand as the optimal site for the placement of the TiO_2 anchoring group [71].

Finally, while as of now there have been no theoretical studies focusing on interactions between the oxidized Fe(II) dyes and redox couples, computational tools for such investigations are readily available [194] and will likely emerge as an area of interest in the near future.

5. Conclusions

Fe(II) complexes hold an intense fascination for chemists, from both a fundamental electronic structure perspective, and for their numerous potential applications for solar energy conversion, molecular electronics, spintronics, and more. The fact that they are also highly challenging to characterize from a computational standpoint only makes them more exciting systems for both theory development, and application-based computational chemistry. The aim of this review was to demonstrate that while there have been major advances in the field, accurately applying electronic structure methods to Fe(II) complexes, especially in the context of spin-state energetics, is still a challenging area of work. It is important to emphasize how critical it is to be aware of, and properly apply different theoretical techniques depending on a method's reliability. *ab initio* methods such as CASPT2 are effective for determining $\Delta E_{HS/LS}$ and excited state features, but they are highly impractical for determining molecular structure or other important thermochemical components. DFT on the other hand generally cannot be counted on to determine $\Delta E_{HS/LS}$, but can handle geometry optimization, frequency calculation, and spectroscopic simulation (via TD-DFT) effectively, and certainly on a massively more affordable scale than *ab initio* methods. Through careful analysis of DFT's well-documented flaws it is still possible to use it for qualitative understanding of what features effect $\Delta E_{HS/LS}$, especially when done in tandem with higher-level calculations or through utilization of experimental benchmarks. Electronic structure calculations are the most powerful when utilized together with experiments to explain, corroborate, or predict the results of experimental studies as was demonstrated in numerous examples of such combined studies on LIESST and photodecay of excited Fe(II) complexes. While there are still many wrinkles to be ironed out for electronic structure calculations of Fe(II) systems, based on the current progress of theory development and successful coordination with experimentalists the future looks brighter than ever.

Notes

The authors declare no competing financial interest.

Acknowledgments

This work was supported by the National Science Foundation grant CH-1554855.

References

[1] H.-K. Liu, P.J. Sadler, Acc. Chem. Res. 44 (2011) 349–359.
[2] H.T. Chifotides, K.R. Dunbar, Acc. Chem. Res. 38 (2005) 146–156.
[3] W. Liu, R. Gust, Chem. Soc. Rev. 42 (2013) 755–773.
[4] M. Aresta, A. Dibenedetto, A. Angelini, Chem. Rev. 114 (2014) 1709–1742.
[5] W.-H. Wang, Y. Himeda, J.T. Muckerman, G.F. Manbeck, E. Fujita, Chem. Rev. 115 (2015) 12936–12973.
[6] M. Cokoja, C. Bruckmeier, B. Rieger, W.A. Herrmann, F.E. Kuhn, Angew. Chem. Int. Ed. 50 (2011) 8510–8537.
[7] K. Huang, C.L. Sun, Z.J. Shi, Chem. Soc. Rev. 40 (2011) 2435–2452.
[8] H. Dau, C. Limberg, T. Reier, M. Risch, S. Roggan, P. Strasser, ChemCatChem 2 (2010) 724–761.
[9] A. Singh, L. Spiccia, Coord. Chem. Rev. 257 (2013) 2607–2622.
[10] L. Tong, R.P. Thummel, Chem. Sci. 7 (2016) 6591–6603.
[11] J.D. Blakemore, R.H. Crabtree, G.W. Brudvig, Chem. Rev. 115 (2015) 12974–13005.
[12] S. Romain, L. Vigara, A. Llobet, Acc. Chem. Res. 42 (2009) 1944–1953.
[13] X. Zhang, L.W. Chung, Y.D. Wu, Acc. Chem. Res. 49 (2016) 1302–1310.
[14] T. Gensch, M.N. Hopkinson, F. Glorius, J. Wencel-Delord, Chem. Soc. Rev. 45 (2016) 2900–2936.
[15] X. Chen, K.M. Engle, D.H. Wang, J.Q. Yu, Angew. Chem. Int. Ed. 48 (2009) 5094–5115.
[16] V. Ritleng, C. Sirlin, M. Pfeffer, Chem. Rev. 102 (2002) 1731–1770.
[17] I.A.I. Mkhalid, J.H. Barnard, T.B. Marder, J.M. Murphy, J.F. Hartwig, Chem. Rev. 110 (2010) 890–931.
[18] W. Guan, F.B. Sayyed, G. Zeng, S. Sakaki, Inorg. Chem. 53 (2014) 6444–6457.
[19] Z. Shao, H. Zhang, Chem. Soc. Rev. 38 (2009) 2745–2755.
[20] J.F. Hartwig, Nature 455 (2008) 314–322.
[21] C.K. Prier, D.A. Rankic, D.W. MacMillan, Chem. Rev. 113 (2013) 5322–5363.
[22] C.J. Cramer, D.G. Truhlar, Phys. Chem. Chem. Phys. 11 (2009) 10757–10816.
[23] A.J. Esswein, D.G. Nocera, Chem. Rev. 107 (2007) 4022–4047.
[24] K. Sonogashira, J. Organomet. Chem. 653 (2002) 46–49.
[25] K.H. Jensen, M.S. Sigman, Org. Biomol. Chem. 6 (2008) 4083.
[26] U. Christmann, R.N. Vilar, Angew. Chem. Int. Ed. 44 (2005) 366–374.
[27] J.A. Labinger, Chem. Rev. (2016), http://dx.doi.org/10.1021/acs.chemrev.6b00583.
[28] Y. Park, S. Ahn, D. Kang, M.-H. Baik, Acc. Chem. Res. 49 (2016) 1263–1270.
[29] S. Enthaler, K. Junge, M. Beller, Angew. Chem. Int. Ed. 47 (2008) 3317–3321.
[30] P. Gamez, J.S. Costa, M. Quesada, G. Aromi, Dalton Trans. (2009) 7845–7853.
[31] O. Sato, J. Tao, Y.Z. Zhang, Angew. Chem. Int. Ed. 46 (2007) 2152–2187.
[32] A. Bousseksou, G. Molnár, G. Matouzenko, Eur. J. Inorg. Chem. 2004 (2004) 4353–4369.
[33] A.B. Gaspar, V. Ksenofontov, M. Seredyuk, P. Gütlich, Coord. Chem. Rev. 249 (2005) 2661–2676.
[34] B. Su, Z.C. Cao, Z.J. Shi, Acc. Chem. Res. 48 (2015) 886–896.
[35] I. Bauer, H.J. Knolker, Chem. Rev. 115 (2015) 3170–3387.
[36] A. Fürstner, ACS Cent. Sci. (2016).
[37] C. Bolm, J. Legros, J. Le Paih, L. Zani, Chem. Rev. 104 (2004) 6217–6254.
[38] T.G. Gopakumar, F. Matino, H. Naggert, A. Bannwarth, F. Tuczek, R. Berndt, Angew. Chem. Int. Ed. 51 (2012) 6262–6266.
[39] I. Žutić, J. Fabian, S. Das Sarma, Rev. Mod. Phys. 76 (2004) 323–410.
[40] J. Harvey, Coord. Chem. Rev. 238–239 (2003) 347–361.
[41] D. Schröder, S. Shaik, H. Schwarz, Acc. Chem. Res. 33 (2000) 139–145.
[42] S. Shaik, D. Danovich, A. Fiedler, D. Schröder, H. Schwarz, Helv. Chim. Acta 78 (1995) 1393–1407.
[43] D. Mandal, S. Shaik, J. Am. Chem. Soc. 138 (2016) 2094–2097.
[44] Y. Sun, H. Tang, K. Chen, L. Hu, J. Yao, S. Shaik, H. Chen, J. Am. Chem. Soc. 138 (2016) 3715–3730.
[45] S. Shaik, S.P. de Visser, F. Ogliaro, H. Schwarz, D. Schröder, Curr. Opin. Chem. Biol. 6 (2002) 556–567.
[46] G. Brehm, M. Reiher, S. Schneider, J. Phys. Chem. A 106 (2002) 12024–12034.
[47] A. Rudavskyi, C. Sousa, C. de Graaf, R.W. Havenith, R. Broer, J. Chem. Phys. 140 (2014) 184318.
[48] M. Sorai, S. Seki, J. Phys. Chem. Solids 35 (1974) 555–570.
[49] K.P. Kepp, Inorg. Chem. 55 (2016) 2717–2727.
[50] K. Andersson, P.A. Malmqvist, B.O. Roos, J. Chem. Phys. 96 (1992) 1218–1226.
[51] K. Andersson, P.A. Malmqvist, B.O. Roos, A.J. Sadlej, K. Wolinski, J. Phys. Chem. 94 (1990) 5483–5488.
[52] P.Å. Malmqvist, K. Pierloot, A.R.M. Shahi, C.J. Cramer, L. Gagliardi, J. Chem. Phys. 128 (2008) 204109.
[53] P. Hohenberg, W. Kohn, Phys. Rev. 136 (1964) B864–B871.
[54] W. Kohn, L.J. Sham, Phys. Rev. 140 (1965) A1133–A1138.
[55] J.A. Real, A.B. Gaspar, V. Niel, M.C. Muñoz, Coord. Chem. Rev. 236 (2003) 121–141.
[56] A. Hauser, J. Jeftić, H. Romstedt, R. Hinek, H. Spiering, Coord. Chem. Rev. 190–192 (1999) 471–491.
[57] M.A. Halcrow, Polyhedron 26 (2007) 3523–3576.
[58] H. Paulsen, V. Schünemann, J.A. Wolny, Eur. J. Inorg. Chem. 2013 (2013) 628–641.
[59] D.S. Middlemiss, R.J. Deeth, J. Chem. Phys. 140 (2014), 144503-1–144503-7.
[60] D.S. Middlemiss, D. Portinari, C.P. Grey, C.A. Morrison, C.C. Wilson, Phys. Rev. B 81 (2010) 184410.
[61] B. O'Regan, M. Gratzel, Nature 353 (1991) 737–740.
[62] A. Hagfeldt, G. Boschloo, L. Sun, L. Kloo, H. Pettersson, Chem. Rev. 110 (2010) 6595–6663.
[63] E. Jakubikova, D.N. Bowman, Acc. Chem. Res. 48 (2015) 1441–1449.
[64] S. Ardo, G.J. Meyer, Chem. Soc. Rev. 38 (2009) 115–164.
[65] W. Henry, C.G. Coates, C. Brady, K.L. Ronayne, P. Matousek, M. Towrie, S.W. Botchway, A.W. Parker, J.G. Vos, W.R. Browne, J.J. McGarvey, J. Phys. Chem. A 112 (2008) 4537–4544.
[66] J.E. Monat, J.K. McCusker, J. Am. Chem. Soc. 122 (2000) 4092–4097.

[67] W. Zhang, R. Alonso-Mori, U. Bergmann, C. Bressler, M. Chollet, A. Galler, W. Gawelda, R.G. Hadt, R.W. Hartsock, T. Kroll, K.S. Kjaer, K. Kubicek, H.T. Lemke, H.W. Liang, D.A. Meyer, M.M. Nielsen, C. Purser, J.S. Robinson, E.I. Solomon, Z. Sun, D. Sokaras, T.B. van Driel, G. Vanko, T.C. Weng, D. Zhu, K.J. Gaffney, Nature 509 (2014) 345–348.
[68] Y. Liu, T. Harlang, S.E. Canton, P. Chabera, K. Suarez-Alcantara, A. Fleckhaus, D. A. Vithanage, E. Goransson, A. Corani, R. Lomoth, V. Sundstrom, K. Warnmark, Chem. Commun. 49 (2013) 6412–6414.
[69] L.A. Fredin, M. Pápai, E. Rozsályi, G. Vankó, K. Wärnmark, V. Sundström, P. Persson, J. Phys. Chem. Lett. 5 (2014) 2066–2071.
[70] T.C.B. Harlang, Y. Liu, O. Gordivska, L.A. Fredin, C.S. Ponseca Jr., P. Huang, P. Chábera, K.S. Kjaer, H. Mateos, J. Uhlig, R. Lomoth, R. Wallenberg, S. Styring, P. Persson, V. Sundström, K. Wärnmark, Nat. Chem. 7 (2015) 883–889.
[71] S. Mukherjee, D.N. Bowman, E. Jakubikova, Inorg. Chem. 54 (2015) 560–569.
[72] S.G. Shepard, S.M. Fatur, A.K. Rappe, N.H. Damrauer, J. Am. Chem. Soc. 138 (2016) 2949–2952.
[73] L.A. Büldt, X. Guo, R. Vogel, A. Prescimone, O.S. Wenger, J. Am. Chem. Soc. 139 (2017) 985–992.
[74] A. Hauser, Light-induced spin crossover and the high-spin→low-spin relaxation, in: P. Gütlich, H.A. Goodwin (Eds.), Spin Crossover in Transition Metal Compounds II, Springer, Berlin Heidelberg, Berlin, Heidelberg, 2004, pp. 155–198.
[75] J.N. Harvey, Struct. Bond. 112 (2004) 151–184.
[76] F. Neese, Coord. Chem. Rev. 253 (2009) 526–563.
[77] J.N. Harvey, Annu. Rep. Prog. Chem. Sect. C: Phys. Chem. 102 (2006) 203.
[78] J. Autschbach, J. Chem. Phys. 136 (2012), 150902-150902-150915..
[79] F. Neese, T. Petrenko, D. Ganyushin, G. Olbrich, Coord. Chem. Rev. 251 (2007) 288–327.
[80] P. Geerlings, F. De Proft, W. Langenaeker, Chem. Rev. 103 (2003) 1793–1874.
[81] A.D. Becke, J. Chem. Phys. 140 (2014) 18A301.
[82] T. Helgaker, S. Coriani, P. Jørgensen, K. Kristensen, J. Olsen, K. Ruud, Chem. Rev. 112 (2012) 543–631.
[83] J.A. Pople, Rev. Mod. Phys. 71 (1999) 1267–1274.
[84] S.F. Sousa, P.A. Fernandes, M.J. Ramos, J. Phys. Chem. A 111 (2007) 10439–10452.
[85] K. Burke, J. Chem. Phys. 136 (2012) 150901.
[86] M.W. Schmidt, M.S. Gordon, Annu. Rev. Phys. Chem. 49 (1998) 233.
[87] C.J. Stein, M. Reiher, J. Chem. Theory Comput. 12 (2016) 1760–1771.
[88] V. Veryazov, P.Å. Malmqvist, B.O. Roos, Int. J. Quantum Chem. 111 (2011) 3329–3338.
[89] K. Pierloot, S. Vancoillie, J. Chem. Phys. 125 (2006) 124303.
[90] R.K. Carlson, S.O. Odoh, S.J. Tereniak, C.C. Lu, L. Gagliardi, J. Chem. Theory Comput. 11 (2015) 4093–4101.
[91] K. Pierloot, in: T.R. Cundari (Ed.), Computational Organometallic Chemistry, Dekker, New York, 2001.
[92] K. Pierloot, Mol. Phys. 101 (2003) 2083–2094.
[93] S.R. White, Phys. Rev. Lett. 69 (1992) 2863–2866.
[94] S.R. White, Phys. Rev. B 48 (1993) 10345–10356.
[95] Y. Kurashige, T. Yanai, J. Chem. Phys. 135 (2011) 094104.
[96] S. Guo, M.A. Watson, W. Hu, Q. Sun, G.K. Chan, J. Chem. Theory Comput. 12 (2016) 1583–1591.
[97] K.H. Marti, I.M. Ondík, G. Moritz, M. Reiher, J. Chem. Phys. 128 (2008) 014104.
[98] Q.M. Phung, S. Wouters, K. Pierloot, J. Chem. Theory Comput. 12 (2016) 4352–4361.
[99] D. Ma, G. Li Manni, L. Gagliardi, J. Chem. Phys. 135 (2011) 044128.
[100] D. Ma, G. Li Manni, J. Olsen, L. Gagliardi, J. Chem. Theory Comput. 12 (2016) 3208–3213.
[101] M. Radon, E. Broclawik, K. Pierloot, J. Chem. Theory Comput. 7 (2011) 898–908.
[102] S. Vancoillie, H. Zhao, V.T. Tran, M.F. Hendrickx, K. Pierloot, J. Chem. Theory Comput. 7 (2011) 3961–3977.
[103] C.J. Stein, V. von Burg, M. Reiher, J. Chem. Theory Comput. 12 (2016) 3764–3773.
[104] M. Pápai, G. Vankó, C. de Graaf, T. Rozgonyi, J. Chem. Theory Comput. 9 (2013) 509–519.
[105] C. Camacho, H.A. Witek, S. Yamamoto, J. Comput. Chem. 30 (2009) 468–478.
[106] C. Camacho, R. Cimiraglia, H.A. Witek, Phys. Chem. Chem. Phys. 12 (2010) 5058–5060.
[107] J. Soto, F.J. Avila, J.C. Otero, J.F. Arenas, Phys. Chem. Chem. Phys. 13 (2011) 7230–7231.
[108] G. Ghigo, B.O. Roos, P.-Å. Malmqvist, Chem. Phys. Lett. 396 (2004) 142–149.
[109] M. Kepenekian, V. Robert, B. Le Guennic, J. Chem. Phys. 131 (2009) 114702.
[110] N. Suaud, M.-L. Bonnet, C. Boilleau, P. Labèguerie, N. Guihéry, J. Am. Chem. Soc. 131 (2009) 715–722.
[111] L.M. Lawson Daku, F. Aquilante, T.W. Robinson, A. Hauser, J. Chem. Theory Comput. 8 (2012) 4216–4231.
[112] C. Angeli, R. Cimiraglia, Theor. Chem. Acc. 107 (2002) 313–317.
[113] C. Angeli, R. Cimiraglia, S. Evangelisti, T. Leininger, J.P. Malrieu, J. Chem. Phys. 114 (2001) 10252.
[114] C. Angeli, R. Cimiraglia, J.-P. Malrieu, Chem. Phys. Lett. 350 (2001) 297–305.
[115] C. Angeli, R. Cimiraglia, J.-P. Malrieu, J. Chem. Phys. 117 (2002) 9138.
[116] I. Schapiro, K. Sivalingam, F. Neese, J. Chem. Theory Comput. 9 (2013) 3567–3580.
[117] N. Queralt, D. Taratiel, C. de Graaf, R. Caballol, R. Cimiraglia, C. Angeli, J. Comput. Chem. 29 (2008) 994–1003.
[118] L. Freitag, S. Knecht, C. Angeli, M. Reiher, J. Chem. Theory Comput. (2017), http://dx.doi.org/10.1021/acs.jctc.6b00778.
[119] M. Fumanal, L.K. Wagner, S. Sanvito, A. Droghetti, J. Chem. Theory Comput. 12 (2016) 4233–4241.
[120] E.D. Hedegard, S. Knecht, J.S. Kielberg, H.J. Jensen, M. Reiher, J. Chem. Phys. 142 (2015) 224108.
[121] E. Fromager, J. Toulouse, H.J. Jensen, J. Chem. Phys. 126 (2007) 074111.
[122] J.D. Goodpaster, T.A. Barnes, F.R. Manby, T.F. Miller 3rd, J. Chem. Phys. 137 (2012) 224113.
[123] J.D. Goodpaster, T.A. Barnes, F.R. Manby, T.F. Miller 3rd, J. Chem. Phys. 140 (2014) 18A507.
[124] J.L. Bao, A. Sand, L. Gagliardi, D.G. Truhlar, J. Chem. Theory Comput. 12 (2016) 4274–4283.
[125] G. Li Manni, R.K. Carlson, S. Luo, D. Ma, J. Olsen, D.G. Truhlar, L. Gagliardi, J. Chem. Theory Comput. 10 (2014) 3669–3680.
[126] S. Pijeau, E.G. Hohenstein, J. Chem. Theory Comput. (2017), http://dx.doi.org/10.1021/acs.jctc.6b00893.
[127] A.D. Becke, J. Chem. Phys. 98 (1993) 5648–5652.
[128] J.P. Perdew, A. Ruzsinszky, J. Tao, V.N. Staroverov, G.E. Scuseria, G.I. Csonka, J. Chem. Phys. 123 (2005) 62201.
[129] A. Domingo, M. Àngels Carvajal, C. de Graaf, Int. J. Quantum Chem. 110 (2010) 331–337.
[130] M. Reiher, O. Salomon, B. Artur Hess, Theor. Chem. Acc. 107 (2001) 48–55.
[131] H. Paulsen, L. Duelund, H. Winkler, H. Toftlund, A.X. Trautwein, Inorg. Chem. 40 (2001) 2201–2203.
[132] A. Ghosh, P.R. Taylor, Curr. Opin. Chem. Biol. 7 (2003) 113–124.
[133] J. Conradie, A. Ghosh, J. Phys. Chem. B 111 (2007) 12621–12624.
[134] A. Ghosh, J. Biol. Inorg. Chem. 11 (2006) 712–724.
[135] A. Ghosh, T. Vangberg, E. Gonzalez, P. Taylor, J. Porphyrins Phthalocyanines 5 (2001) 345–356.
[136] F. De Angelis, N. Jin, R. Car, J.T. Groves, Inorg. Chem. 45 (2006) 4268–4276.
[137] C. Rong, S. Lian, D. Yin, B. Shen, A. Zhong, L. Bartolotti, S. Liu, J. Chem. Phys. 125 (2006) 174102.
[138] M. Reiher, Inorg. Chem. 41 (2002) 6928–6935.
[139] O. Salomon, M. Reiher, B.A. Hess, J. Chem. Phys. 117 (2002) 4729–4737.
[140] R.L. Lord, F.A. Schultz, M.-H. Baik, J. Am. Chem. Soc. 131 (2009) 6189–6197.
[141] M. Domarus, M.L. Kuznetsov, J. Marçalo, A.J.L. Pombeiro, J.A.L. da Silva, Angew. Chem. Int. Ed. 55 (2016) 1489–1492.
[142] M. Leibold, S. Kisslinger, F.W. Heinemann, F. Hampel, Y. Ichiyanagi, M. Klein, P. Homenya, F. Renz, H. Toftlund, G. Brehm, S. Schneider, M. Reiher, S. Schindler, Z. Anorg. Allg. Chem. 642 (2016) 85–94.
[143] M. Pápai, T.J. Penfold, K.B. Møller, J. Phys. Chem. C 120 (2016) 17234–17241.
[144] A.A. Starikova, D.V. Steglenko, A.G. Starikov, V.I. Minkin, Dokl. Chem. 468 (2016) 152–155.
[145] H. Wang, H. Wang, R.B. King, H.F. Schaefer 3rd, J. Comput. Chem. 37 (2016) 250–260.
[146] J.-L. Carreón-Macedo, J.N. Harvey, J. Am. Chem. Soc. 126 (2004) 5789–5797.
[147] V.W. Manner, A.D. Lindsay, E.A. Mader, J.N. Harvey, J.M. Mayer, Chem. Sci. 3 (2012) 230.
[148] S. Zein, S.A. Borshch, P. Fleurat-Lessard, M.E. Casida, H. Chermette, J. Chem. Phys. 126 (2007) 014105.
[149] D.N. Bowman, E. Jakubikova, Inorg. Chem. 51 (2012) 6011–6019.
[150] E.I. Ioannidis, H.J. Kulik, J. Phys. Chem. A 121 (2017) 874–884.
[151] S. Grimme, J. Chem. Phys. 124 (2006) 034108.
[152] S. Ye, F. Neese, Inorg. Chem. 49 (2010) 772–774.
[153] A. Slimani, X. Yu, A. Muraoka, K. Boukheddaden, K. Yamashita, J. Phys. Chem. A 118 (2014) 9005–9012.
[154] E. Runge, E.K.U. Gross, Phys. Rev. Lett. 52 (1984) 997–1000.
[155] C. Adamo, D. Jacquemin, Chem. Soc. Rev. 42 (2013) 845–856.
[156] M.E. Casida, M. Huix-Rotllant, Annu. Rev. Phys. Chem. 63 (2012) 287–323.
[157] A. Rosa, G. Ricciardi, O. Gritsenko, E. Baerends, Excitation energies of metal complexes with time-dependent density functional theory, in: Principles and Applications of Density Functional Theory in Inorganic Chemistry I, Springer, Berlin Heidelberg, 2004, pp. 49–116.
[158] A.D. Laurent, C. Adamo, D. Jacquemin, Phys. Chem. Chem. Phys. 16 (2014) 14334–14356.
[159] T. Le Bahers, E. Bremond, I. Ciofini, C. Adamo, Phys. Chem. Chem. Phys. 16 (2014) 14435–14444.
[160] L.M. Lawson Daku, A. Vargas, A. Hauser, A. Fouqueau, M.E. Casida, ChemPhysChem 6 (2005) 1393–1410.
[161] G. Ganzenmuller, N. Berkaine, A. Fouqueau, M.E. Casida, M. Reiher, J. Chem. Phys. 122 (2005) 234321.
[162] E.I. Ioannidis, H.J. Kulik, J. Chem. Phys. 143 (2015) 034104.
[163] T.F. Hughes, R.A. Friesner, J. Chem. Theory Comput. 7 (2011) 19–32.
[164] K. Pierloot, S. Vancoillie, J. Chem. Phys. 128 (2008) 034104.
[165] H. Paulsen, L. Duelund, H. Winkler, H. Toftlund, H.X. Trautwein, Inorg. Chem. 40 (2001) 2201–2203.
[166] L.J. Kershaw Cook, R. Kulmaczewski, R. Mohammed, S. Dudley, S.A. Barrett, M. A. Little, R.J. Deeth, M.A. Halcrow, Angew. Chem. Int. Ed. 55 (2016) 4327–4331.
[167] I.M. Dixon, F. Alary, M. Boggio-Pasqua, J.L. Heully, Inorg. Chem. 52 (2013) 13369–13374.
[168] I.M. Dixon, S. Khan, F. Alary, M. Boggio-Pasqua, J.L. Heully, Dalton Trans. 43 (2014) 15898–15905.
[169] I.M. Dixon, G. Boissard, H. Whyte, F. Alary, J.L. Heully, Inorg. Chem. 55 (2016) 5089–5091.

[170] D.N. Bowman, A. Bondarev, S. Mukherjee, E. Jakubikova, Inorg. Chem. 54 (2015) 8786–8793.
[171] L.L. Jamula, A.M. Brown, D. Guo, J.K. McCusker, Inorg. Chem. 53 (2014) 15–17.
[172] W. Zhang, K.S. Kjaer, R. Alonso-Mori, U. Bergmann, M. Chollet, L.A. Fredin, R.G. Hadt, R.W. Hartsock, T. Harlang, T. Kroll, K. Kubicek, H.T. Lemke, H.W. Liang, Y. Liu, M.M. Nielsen, P. Persson, J.S. Robinson, E.I. Solomon, Z. Sun, D. Sokaras, T.B. van Driel, T.C. Weng, D. Zhu, K. Warnmark, V. Sundstrom, K.J. Gaffney, Chem. Sci. (2017).
[173] K. Pierloot, E. Van Praet, L.G. Vanquickenborne, B.O. Roos, J. Phys. Chem. 97 (1993) 12220–12228.
[174] A.L. Formiga, S. Vancoillie, K. Pierloot, Inorg. Chem. 52 (2013) 10653–10663.
[175] N. Huse, H. Cho, K. Hong, L. Jamula, F.M.F. de Groot, T.K. Kim, J.K. McCusker, R. W. Schoenlein, J. Phys. Chem. Lett. 2 (2011) 880–884.
[176] A.L. Smeigh, M. Creelman, R.A. Mathies, J.K. McCusker, J. Am. Chem. Soc. 130 (2008) 14105–14107.
[177] E.A. Juban, A.L. Smeigh, J.E. Monat, J.K. McCusker, Coord. Chem. Rev. 250 (2006) 1783–1791.
[178] W. Gawelda, A. Cannizzo, V.-T. Pham, F. van Mourik, C. Bressler, M. Chergui, J. Am. Chem. Soc. 129 (2007) 8199–8206.
[179] C. Bressler, C. Milne, V.-T. Pham, A. ElNahhas, R.M. van der Veen, W. Gawelda, S. Johnson, P. Beaud, D. Grolimund, M. Kaiser, C.N. Borca, G. Ingold, R. Abela, M. Chergui, Science 323 (2009) 489–492.
[180] C.D. Graaf, C. Sousa, Int. J. Quantum Chem. 111 (2011) 3385–3393.
[181] J. Chang, A. Fedro, M. van Veenendaal, Phys. Rev. B 82 (2010).
[182] M. van Veenendaal, J. Chang, A.J. Fedro, Phys. Rev. Lett. 104 (2010).
[183] W. Zhang, K.J. Gaffney, Acc. Chem. Res. 48 (2015) 1140–1148.
[184] J.K. McCusker, Nat. Phys. 10 (2014) 476–477.
[185] A. Moguilevski, M. Wilke, G. Grell, S.I. Bokarev, S.G. Aziz, N. Engel, A.A. Raheem, O. Kühn, I.Y. Kiyan, E.F. Aziz, ChemPhysChem (2017), http://dx.doi.org/10.1002/cphc.201601396.
[186] B. Ordejon, C. de Graaf, C. Sousa, J. Am. Chem. Soc. 130 (2008) 13961–13968.
[187] C. deGraaf, C. Sousa, Chem. Eur. J. 16 (2010) 4550–4556.
[188] C. Sousa, C. de Graaf, A. Rudavskyi, R. Broer, J. Tatchen, M. Etinski, C.M. Marian, Chem. Eur. J. 19 (2013) 17541–17551.
[189] J. Nance, D.N. Bowman, S. Mukherjee, C.T. Kelley, E. Jakubikova, Inorg. Chem. 54 (2015) 11259–11268.
[190] S.E. Canton, X. Zhang, M.L. Lawson Daku, Y. Liu, J. Zhang, S. Alvarez, J. Phys. Chem. C 119 (2015) 3322–3330.
[191] Y. Liu, P. Persson, V. Sundstrom, K. Warnmark, Acc. Chem. Res. 49 (2016) 1477–1485.
[192] T.C. Motley, G.J. Meyer, NPG Asia Mater. 8 (2016) e261.
[193] E. Galoppini, Nat. Chem. 7 (2015) 861–862.
[194] E. Mosconi, J.H. Yum, F. Kessler, C.J. Gomez Garcia, C. Zuccaccia, A. Cinti, M.K. Nazeeruddin, M. Gratzel, F. De Angelis, J. Am. Chem. Soc. 134 (2012) 19438–19453.
[195] J.P. Muscat, D.M. Newns, Prog. Surf. Sci. 9 (1978) 1–43.
[196] P.W. Anderson, Phys. Rev. 124 (1961) 41–53.
[197] P. Persson, S. Lunell, L. Ojamäe, Chem. Phys. Lett. 364 (2002) 469–474.
[198] L.G.C. Rego, V.S. Batista, J. Am. Chem. Soc. 125 (2003) 7989–7997.
[199] M. Pastore, T. Duchanois, L. Liu, A. Monari, X. Assfeld, S. Haacke, P.C. Gros, Phys. Chem. Chem. Phys. 18 (2016) 28069–28081.
[200] L.A. Fredin, K. Wärnmark, V. Sundström, P. Persson, ChemSusChem 9 (2016) 667–675.
[201] D.N. Bowman, J.H. Blew, T. Tsuchiya, E. Jakubikova, Inorg. Chem. 52 (2013) 8621–8628.
[202] D.N. Bowman, J.H. Blew, T. Tsuchiya, E. Jakubikova, Inorg. Chem. 52 (2013), 14449-14449.
[203] D.N. Bowman, S. Mukherjee, L.J. Barnes, E. Jakubikova, J. Phys.: Condens. Matter 27 (2015) 134205.
[204] S. Ferrere, B.A. Gregg, J. Am. Chem. Soc. 120 (1998) 843–844.